A NOVEL APPROACH

USING TENDON VIBRATION

TO STUDY

SPINAL REFLEXES

By

KENNETH TSANG, B.ENG.

A Thesis

Submitted to the School of Graduate Studies

in Partial Fulfilment of the Requirements

for the Degree

Master of Applied Science

McMaster University

MASTER OF APPLIED SCIENCE (2008)   McMaster University

Hamilton, Ontario

TITLE: A Novel Approach using Tendon Vibration to study Spinal Reflexes

AUTHOR: Kenneth Tsang, B.ENG. (McMaster University)

SUPERVISOR: Dr. Hubert de Bruin

NUMBER OF PAGES: 101

ABSTRACT

Although most muscle spindle investigations have used the cat model and invasive surgical measurement techniques, several investigators have used microneurography to record from the Ia and II fibres in humans during tendon vibration. In these studies the muscle spindle primary (Ia) endings are stimulated using transverse vibration of the tendon at reflex sub-threshold amplitudes. Others have used low amplitude vibration and the H-reflex (monosynaptic electrical response) to determine reflex properties during both agonist and antagonist voluntary contractions. Both of these methods explore only certain parts of the monosynaptic reflex arc; microneurography focus on the properties and firing characteristics of the muscle spindles themselves, whereas the H-reflex response to vibration is a representation of the response of the spinal cord as well as the muscle spindles.

In the past we have developed a PC based instrument that uses LabVIEW and a linear servomotor to study tendon reflex properties by recording H-reflexes (or stretch reflexes for mechanical stimuli) from single tendon taps or electrical stimuli to the afferent nerve. In this thesis we describe a further development of this system to provide precise vibrations of the tendon at up to 55 Hz with amplitudes up to 4 mm. The resultant vibration stretch reflex train is extracted from 2 major background noise sources, 60 Hz power line noise, and vibration artifact noise, of the EMG recording via phase coherent subtractive filtering.

To demonstrate the versatility and efficacy of this system in studying the monosynaptic reflex arc, test results from several pilot studies are presented, using the system to vibrate the human distal flexor carpi radialis tendon: (i) whether stretch reflexes could be entrained with high frequency vibration, as contrary to H-reflexes, (ii) whether the responses were affected by low levels of agonist or antagonist contraction, in agreement with the existing pool of work on the subject using the H-reflex, (iii) whether a separation of the Ia (primary) and II (secondary) ending pathways is observable as individual but delayed responses at low vibration frequencies due to different activation characteristics, and axon diameters, of each ending. Possible physiological mechanisms that explain the resultant behaviour are also discussed.

ACKNOWLEDGEMENTS

This thesis, and the past two years of work it represents, is dedicated first and foremost to my Lord and God, Jesus Christ. I would not have gotten through these past years with the joy and peace that I have been experiencing if it was not for His provision and guidance.

I would like to give my most sincere thanks to Hubert (interestingly in almost 5 years I have never called him anything other than Dr. de Bruin). For all those reassuring moments saying that my work is going just fine; those first months where nothing worked and neither of us knew why; for skipping your morning coffee just so we could get some decent recordings; for just being exactly what I always thought a great graduate advisor should be. Thanks.

My parents and my sister have always supported me in everything that I did. To my parents I owe countless hours of toil throughout the years, and to my sis for simply bearing with me through them. Thanks so much, I would not be here without you.

To my labmates Mike, Faheem, and the bunch at the Biomed Research Lab; you made my working in the office actually sort of fun. Especially to Mike for reminding me of admin things (I probably would have missed quite a few deadlines without you).

Last but not least, to my other family at Westside Hamilton. I know for certain that you are the reason God brought me back to Mac. Thanks for sharing your lives with me. It has been (and hopefully will be) a real joy having you in mine.

TABLE OF CONTENTS

CHAPTER 1
BACKGROUND

1.1   Introduction

This chapter will cover the essentials of muscle anatomy, and proprioceptive physiology, in relation to this particular project. The two main sensory receptors used in proprioception, muscle spindles (MSs) and Golgi Tendon Organs (GTOs), are explored in detail, covering their basic anatomy, function, and innveration (mostly found in the Textbook of Medical Physiology by Guyton, and Principles of Anatomy and Physiology by Totora and Derrickson).

This is followed by a review of various related research in the exploration of the main receptor of influence in spinal reflexes: muscle spindles. Specifically, work using the Hoffman reflex (H-reflex), an electrically induced stimulation of the afferent nerve fibres of muscle spindles, is covered in greater detail, as this is the current clinically prevalent mode of reflex diagnosis. An overview of various excitatory and inhibitory factors of influence to the spinal reflex, and their possible physiological mechanisms, is presented.

As this project proposes a new method of tendon reflex measurement, the chapter concludes with a review of works pertaining to various modes of tendon stimulation, with a focus on the effects of vibration on muscle spindles.

1.2   Muscle Organization and Function

1.2.1   The Motor Unit

The basic functional unit of a muscle is the motor unit, defined as an alpha motor neuron (MN) stemming from the spinal cord, its associated axon, and all of the skeletal muscle fibres that it innervates (Figure 1-1). Each alpha MN may have up to several hundred axon branches that each synapse to a muscle fibre, though anatomically these fibres need not be next to each other in the muscle. This innervation ratio is mainly dictated by the function of the muscle. Muscles that are used for fine movement (such as the thenar muscle which controls the thumb) tend to have fewer fibres per unit, and thus a lower innervation ratio, than larger muscles that are used for more course movements, such as the soleus (plantarflexor of the foot) (Guyton and Hall 2006).
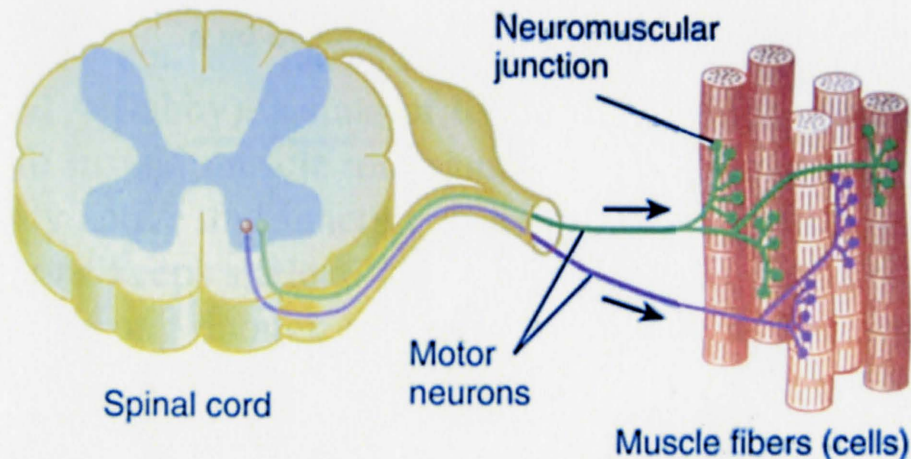

Figure 1-1: 2 motor units are shown, with green and purple alpha MNs respectively. Each unit is comprised of the alpha MN and the muscle fibres it innervates (Tortora and Derrickson 2006).

The recruitment of motor units during a muscle contraction is not entirely random. Typically, for weak contractions, smaller units are recruited first, and the force created is varied via the activation of additional motor units. As the force exerted is increased, larger motor units are recruited, up to 80% of the maximal voluntary contraction (MVC) (De Luca, LeFever et al. 1982). From there MVC is reached by increasing the firing rate of the motor units that are already active (Freund, Budingen et al. 1975). Since the firing of motor units happens asynchronously at the spinal level, a smooth contraction can be achieved utilizing the above modes of variation even for weak contractions using just a few motor units. This recruitment patter is referred to as Hennerman's size principle (Henneman, Somjen et al. 1965), which states that small motor units (those with fewer muscle fibres) are innervated by smaller alpha MNs (with smaller diameter axons), and vice versa. Since small MNs are more excitable, smaller motor units are recruited first.

1.2.2 Motor Unit Action Potentials (MUAPs)

When an alpha motor neuron is activated, a nerve action potential is sent down its axon towards the muscle fibres it innervates (those in this particular motor unit). This potential causes neurotransmitter release at the synapse between the MN and the muscle fibre, an area known as the motor end plate region. The neurotransmitter release will cause the depolarization of the transverse (or T) tubule network, which spreads along the muscle fibre away from the end plate region (Guyton and Hall 2006). This depolarization causes the muscle fibre to contract. Since all of the muscle fibres in a motor unit are

innvervated by the same MN, they contract almost simultaneously. This is referred to as a twitch and could last from a few to as much as 200 ms, depending on whether the fibre is slow or fast twitch type. The maximum force exerted by the motor unit during the twitch occurs between 20 - 150 ms (Kleissen, Buurke et al. 1998). This potential also conducts through the surrounding tissues, eventually reaching the electrode (whether surface or needle) and the resultant measured signal is called a motor unit action potential.

Needle electrodes, due to its close proximity to the muscle fibres, are able to capture this potential as a sharp bi or tri phasic spike, of about 5 ms duration for a single isolated motor unit. With surface electrodes, even with isolation (using nerve truncation for example) the typical spike duration extends to 9-12 ms, due to the different propagation delays introduced by the dispersion of the fibres in the muscle (Basmajian 1980). The larger the MUAP, the larger the motor unit, reason being that the MUAP is the summation of the individual muscle fibre potentials in the motor unit.

1.2.3   Origins of Electromyography (EMG)

In essence, our system measures and processes electromyographic recordings and thus an explanation on the origins of the EMG signal is of relevance. As explained above, the signal recorded by the electrodes originate from the propagation of MUAPs through the surrounding tissue. Since there are many motor units in a muscle, and in light of the motor unit recruitment characteristics mentioned in 1.2.1, the creation of force by a muscle typically involves more than one motor unit firing. Thus the signal recorded by

the electrode is really then a summation of multiple MUAPs (Basmajian 1980; Kleissen, Buurke et al. 1998). This we call the EMG.

The summation of MUAPs can happen in 2 ways. Each muscle fibre can be activated at a higher frequency, or more motor units could be recruited and fire near-simultaneously, as described previously on the topic of force generation. Both of these effects can increase the amplitude of the EMG signal. Since the muscle fibres of different motor units are dispersed throughout the muscle, any surface recorded EMG signals will be both a temporal and spatial summation of different motor unit potentials as units are recruited and their firing characteristics changed according to the contraction in progress, hence the stochastic nature of the EMG signal.

The bandwidth of the EMG signal is estimated to be from 10 to 100 Hz, with the high frequency components occurring during rapid isometric contractions. Slower contractions see the bandwidth reduced to 10 – 40 Hz (Basmajian 1980).

1.3   Proprioceptive Physiology

1.3.1   Basic Description

Two anatomical structures provide proprioceptive sensory information to the spinal cord and cerebral cortex: the muscle spindle and the Golgi tendon organ. These structures, constructed from specialize nervous tissues, are responsible for providing the sensory feedback necessary for cortical and spinal movement control, and also, more relevant to this discussion, for muscle reflexes elicited at the spinal cord.

The muscle spindles (MSs) are placed throughout the muscle belly, and function as a measure of the length, and the rate of change in length, of the muscle. Golgi tendon organs (GTOs) are found within the tendons connecting the muscle to the skeletal structure and are measures of the force, and the rate of change in force, on the muscle in question.

As the monosynaptic reflex arc, the source of the vibration stretch reflex, is a function of the muscle spindle, its anatomy will now be discussed in more detail. A brief description of the GTO will follow.

1.3.2   Muscle Spindles

The general anatomy of the muscle spindle is shown in the top image of Figure 1-2. The main components are the intrafusal muscle fibres, small muscle fibres whose ends are attached to the surrounding normal (extrafusal) muscle fibres. These intrafusal fibres have actin and myosin filaments at their ends only, thus they provide little contractile power. Rather, the stretching of these fibres, corresponding to the stretch in the muscle, stimulates the afferent nerve fibres of the MS, and thus provides a signal of
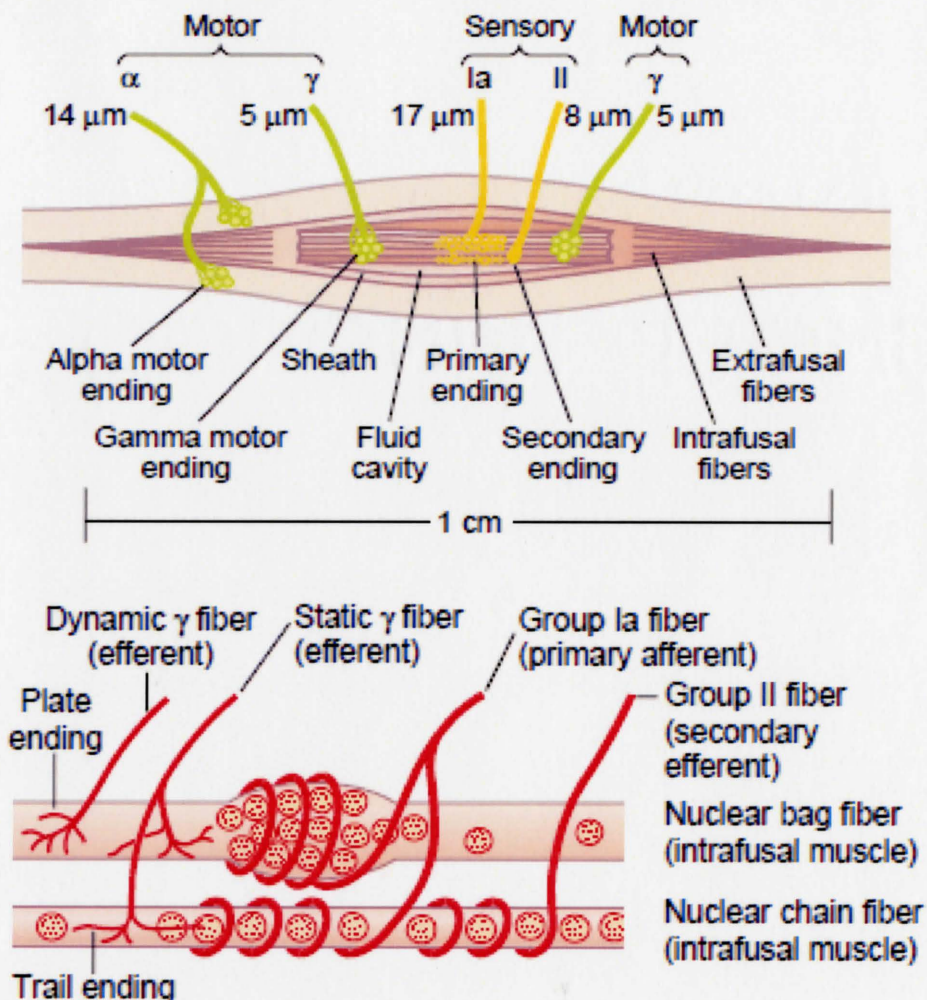

Figure 1-2: Anatomy and physiology of the muscle spindle (Guyton and Hall 2006).

the muscle length and rate of stretch through these nerve fibres. The ends of the intrafusal fibres, however, do have contracting properties, controlled by gamma motor neurons, and are used to keep the fibres taut during length changes in the muscle. This serves to ensure that the MS is properly calibrated as the muscle length changes.

In general, the number of muscle spindles in a particular muscle will depend on the muscle mass and muscle function. Larger muscles tend to have more muscle spindles, with the increase occurring as a power law relation ($y=bx+a$, where y is the log of the number of muscle spindles, and x is the log of the muscle mass) (Kokkorogiannis 2004), Muscles that have a high level of cortical control, such as the muscles that control the fingers (flexor hallucia longus, about 1.7 spindles/g), will have a much higher density of MSs than postural, less voluntary muscles (soleus, 0.94 spindles/g) (Banks 2006).

Two different types of afferent nerve fibres emanate from the midsection of the MS. The group Ia fibre (17 um diameter typical), also known as the primary ending, coils around the midsection of each intrafusal fibre. Type II fibres (8 um diameter typical), or the secondary endings, innervate the MS on either side of the primary ending. As shown in the bottom image of Figure 1-2, there are 2 types of intrafusal fibres, and each type of nerve fibre innervates these differently. Nuclear bag fibres have several nuclei gathered in bags in the midsection of the spindle, while nuclear chain fibres are thinner fibres with nuclei spread in a chain-like fashion. Ia fibres innervate both types, while II fibres only innervate nuclear chain fibres.

If the muscle is slowly stretched, thus the rate of change of the muscle is low, then both endings fire in proportion to the length of the stretch. This increased firing rate will remain for several minutes given the MSs are still being stretched. If the muscle is stretched rapidly, then the frequency of firing of the primary endings will increase dramatically. This increase in frequency only lasts for as long as the muscle's length is increasing. Thus the MSs code for both a static response to signal muscle length, using a steady firing of the secondary endings; and a dynamic response to signal large rate of changes in length, using bursts of impulses in the primary endings.

1.3.3   Golgi Tendon Organs

This sensory receptor is a bundle of 10-15 muscle fibres within the tendon of the muscle, as illustrated in Figure 1-3. The afferent nerve fibres of the GTO are stimulated
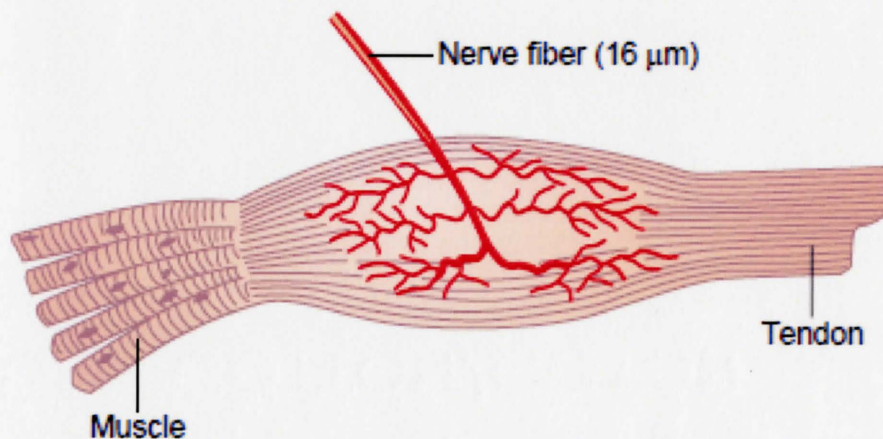

Figure 1-3: Anatomy of the Golgi tendon organ(Guyton and Hall 2006).

when the encapsulated fibres are tensed by the stretching muscle. The GTO acts as a

strain gauge, measuring the tension exerted by the muscle. The resulting signal has the same properties as the signal from Ia fibres: a static response corresponding to slow changes in tension, and a dynamic response corresponding to rapid changes in muscle tension. The GTO, as reflected by research results reviewed later on in this chapter, is utilized in an inhibitory, negative feedback mechanism that prevents the production of excessive force by the muscle fibres. At the extreme, this culminates in the lengthening reaction, where a sudden relaxation of the entire muscle occurs when possible muscle tearing and tendon attachment damage is sensed.

1.4   Monosynaptic reflex arc

1.4.1   Neurocircuitry of the vibration reflex

The basic neuro-circuitry for the monosynaptic reflex arc is shown in Figure 1-4. The components of the arc are the Ia muscle spindle afferent fibres, which synapse onto the homonymous (of the same muscle) alpha MNs, which in turn synapses back onto the muscle. In the figure, we can also see the Ia fibre branching to inhibiting interneurons which synapse onto the alpha MNs of the antagonistics muscles in the same limb, or even onto other muscles of the contralateral limb. The effects of these other connections will be discussed in more detail in a later section. All of this is, of course, an over simplification, as each Ia fibre will synapse onto more than one alpha MN. This grouping of alpha MNs is called the motor neuron pool. This simplification, however, will suffice
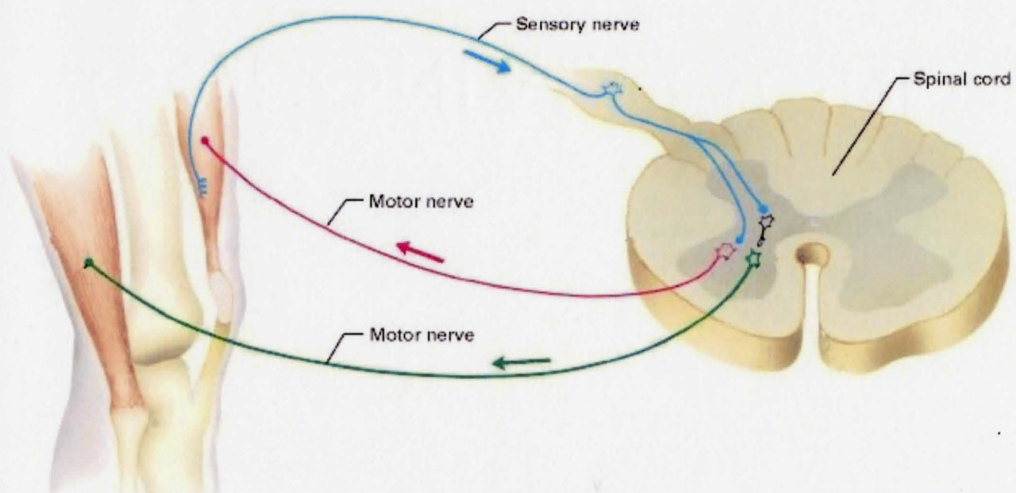

Figure 1-4: Neurocircuit of monosynaptic muscle reflex

at this point of the review to explain the origins of spinal reflexes.

This pathway is used in the muscle stretch reflex, where the muscle spindles described above are stretched due to the stretch in the muscle, via a tendon tap for instance, and cause the Ia afferents to activate. This in turn excites the homonymous alpha MN's to fire, causing the muscle to contract, demonstrating the familiar "jerk" reflex. The same pathway is attributed to the vibration reflex, which is essentially a train of smoother tendon taps.

However, since the Ia afferents synapse onto many different alpha MN's, the input-output relationship between Ia activation and the motor units recruited in the reflex is not quantitatively simple. Rather, many inhibitory and excitatory factors affect the excitability of the motor neuron pool, which then affects the reflex strength exhibited for a certain amount of stimulus amplitude (whether mechanical or electrical). The H wave, detailed in the next sections, the origins of which can be traced to the Ia afferent activation, is a valuable probe in the study of these various factors. It has been used extensively in both clinical diagnostics and research to assess excitability and responses to electrical or mechanical stimuli (Pierrot-Deseilligny and Mazevet 2000), as the stretch vibration reflex is not something that has been extensively studied in published research.

1.4.2 Origins of H-wave

The H-wave results from an electrical stimulus of the motor nerve connecting the muscle of interest to the spinal cord. Figure 1-5 shows the typical wave recorded in H

wave studies. Bipolar surface recording electrodes are placed over the midsection of the muscle. The stimulating electrodes are usually also bipolar, especially for areas where many nerves are located and transverse stimulation is difficult (Pierrot-Deseilligny and Mazevet 2000). Even though transverse stimulation, where the 2 electrodes are placed on opposite sides of the nerve, could be used to elicit an H-reflex with a smaller M-wave contribution (both explained in Figure 1-6 and the paragraphs following), the current required is higher than bipolar electrodes. The stimulating electrodes are placed over the motor nerve of the muscle of interest, the median nerve at the elbow for the FCR for instance.

The recorded waveform reveals 3 distinct sections: the stimulus artifact resulting from tissue volume conduction of the stimulus potential (no time delay), the M-wave due to the direct activation of the alpha MNs by the stimulus and the late H-wave as the stimulus activates Ia afferents which in turn depolarizes the alpha MN, causing the muscle activity reflex as described before. That is, the H-wave is an M-wave elicited
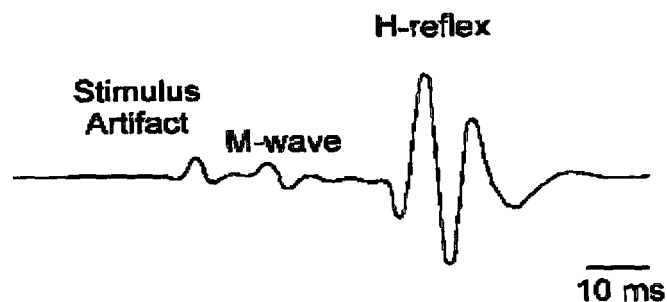
Figure 1-5: Typical recorded H-reflex waveform (Misiaszek 2003)

through the spinal cord, hence the extra time delay.

The comparative amplitudes of the M-wave and H-wave during an H-reflex experiment are inversely proportional as stimulus intensity is increased. Figure 1-6 demonstrates this behaviour (Katz and Pierrot-Deseilligny 1999). When the stimulus
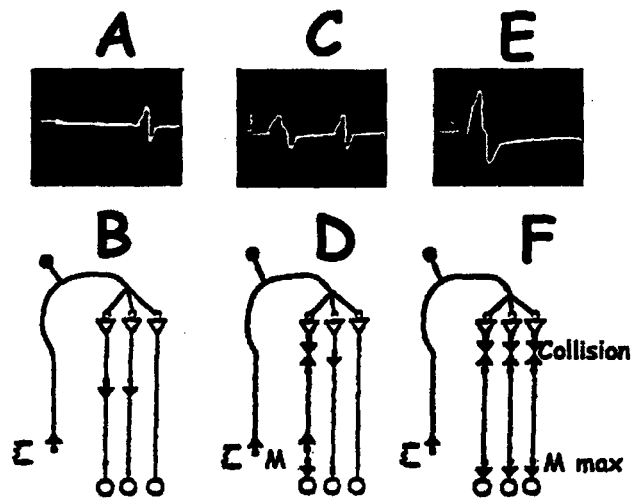

Figure 1-6: H and M-wave amplitudes as stimulus strength increases (Katz and Pierrot-Deseilligny 1999). When the stimulus intensity is low (A-B), only the H-wave is present. As the stimulus intensity is increased (C-D), the amplitude of the M-wave increases and the H-wave is decreased. As the stimulus intensity is increased further (E-F), complete annihilation of the H-wave occurs.

intensity is low (A-B), only the H-wave is present, as the stimulus is too low to recruit the alpha MN's directly, thus only Ia fibres are activated and an H-wave results (usually only possible using transverse stimulation). As the stimulus intensity is increased (C-D), the amplitude of the M-wave increases and the H-wave is decreased. This is due to the stimulus strength being high enough to recruit the MNs and Ia fibres, thus both M-wave and H-wave's are present. The H-wave is decreased primarily due to the antidromic (of

the opposite direction) volleys that are sent centrally from the stimulus. These collide with the descending Ia-induced volleys, and cancel each other, resulting in a reduced recruitment for the H-reflex. These collisions do not totally eliminate the H-wave as the Ia fibres recruit from smaller to larger MNs (Henneman and Mendell 1981), and the electrical stimulus tends to activate larger diameter MNs first (Pierrot-Deseilligny and Mazevet 2000). Thus the M and H-wave will coexist until their respective recruitments overlap and start to collide and cancel the H-wave. As the stimulus intensity is increased further (E-F), complete annihilation of the H-wave occurs as the stimulus creates antidromic volleys in all MNs.
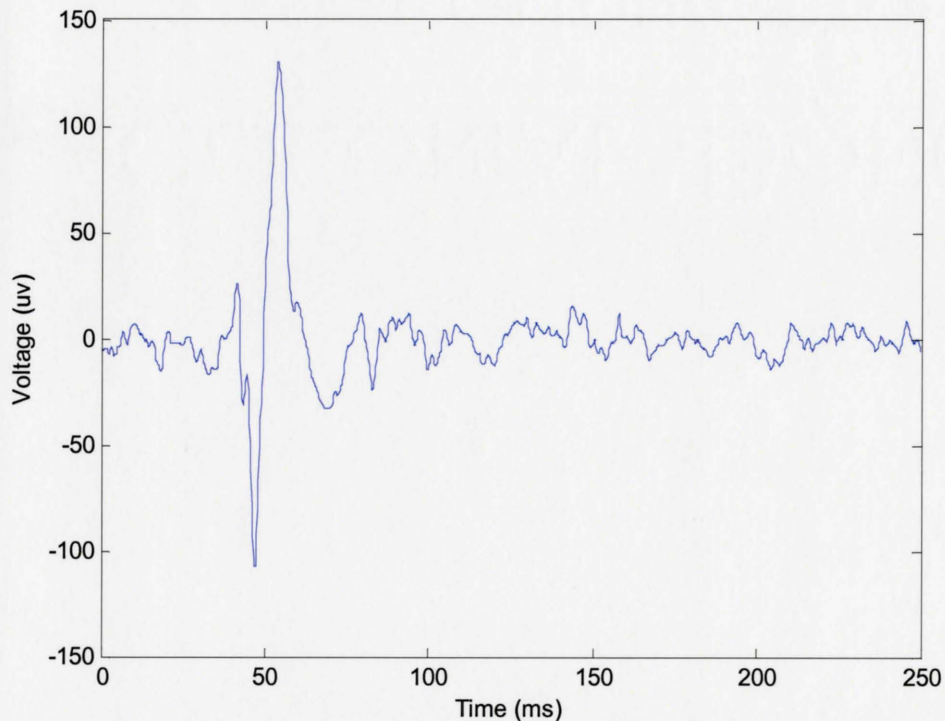

Figure 1-7: Typical response to a single tendon tap, delivered at 0 s.

16

The response for the tendon tap/vibration occurs in a similar fashion: the tap on the tendon stretches the muscle, which stretches the muscles spindles, activating the Ia afferents much like the electrical stimulation. A typical response is shown in Figure 1-7. Note that there is only one section of interest, corresponding to the vibration stretch reflex response, though only for one tap in this instance. This response is analogous to the H-wave. The stimulus artifact and initial M-wave are both absent due to the lack of any electrical stimulus.

1.5   Spinal processing of monosynaptic reflexes

1.5.1   Importance

In addition to the relationships defined above, it is also important to note the various modes of inhibition and excitation that could modulate the H-reflex, and therefore the vibration reflex response. These factors must be accounted for in any experimental method involving these physiological measures to avoid collecting misleading data. These inhibitory and excitatory pathways involve conditioning stimuli from various sources: in homonymous or antagonist muscles, and other muscles on contra (opposite) or ipsilateral (same side) limbs.

1.5.2   Recurrent Inhibition

This is a pathway in which the motor neurons themselves inhibit each other. Alpha MN's, in addition to innervating muscles, also synapse to Renshaw cells. These inhibitory cells are activated by the MNs of synergistic and homonymous muscles, and then synapse back onto the cell body of the alpha and gamma MNs, as well as other Renshaw cells (RCs), causing different realisations of inhibition depending on the movement being performed (Katz and Pierrot-Deseilligny 1999). Figure 1-8 illustrates the relevant connections. The investigation of this pathway was prompted by subjects whose H-wave stopped increasing before their motor threshold was reached (or before the corresponding M-wave was evident), such that the lack of increase cannot be
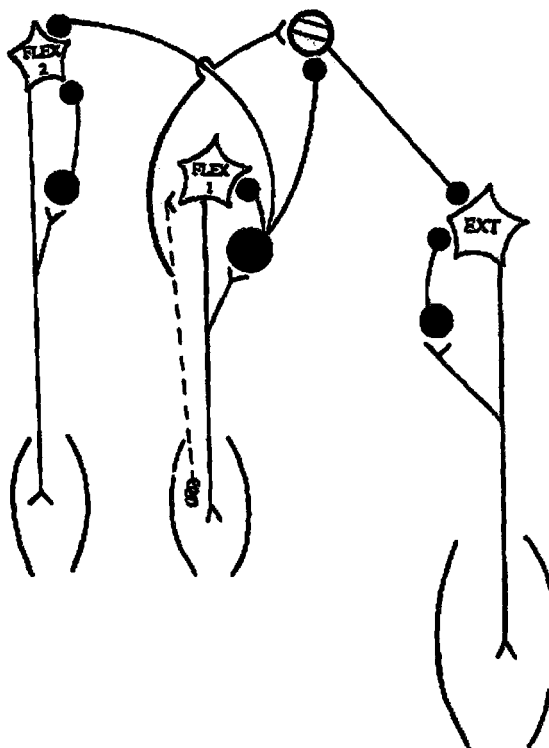
Figure 1-8: The recurrent pathway, solid dots are Renshaw cells, which are innervated by the MNs and synapse back onto the same MNs, or the MNs of other homonymous, or antagonistic muscles (Aymard, Decchi et al. 1997).

attributed to the antidromic volleys. Thus the stimulation itself activated inhibitory mechanisms to limit the reflex response (Pierrot-Deseilligny and Mazevet 2000).

A note of particular interest in recurrent inhibition is the increased level of descending control of the RCs in comparison to the monosynaptic reflex arc. For example, the inhibition of a certain conditioning stimulus varies depending on the voluntary contraction strength of the homonymous muscle (Katz and Pierrot-Deseilligny 1999), indicating additional control upon RCs other than the recurrent synapses mentioned above. There has also been suggestion that this control of recurrent inhibition

is to regulate muscle force and prevent excessive forces (Katz and Pierrot-Deseilligny 1999; Fu 2005).

1.5.3   Post-activation Depression

As with any nervous pathway, the H-reflex cannot be continuously elicited due to, at the very least, the refractory periods of the nerve fibres involved (Burke 2002). However, there is significant evidence that H-reflex depression continues for roughly 8-10 seconds after prior activation of the same Ia fibres (Misiaszek 2003). This depression is significantly dissipated after 3-4s to allow experiments to run at 0.2-0.3Hz (Crone and Nielsen 1989). The depression mechanism is suggested to be reduced neurotransmitter release from the Ia terminals (Hultborn, Illert et al. 1996). The conclusion is in line with intracellular studies of the decerebrate cat's triceps surae. This mechanism is of major importance in designing proper H-reflex studies, as undesired, or unaccounted for, movement could result in length changes of the muscle in question, thereby activating its muscle spindles and corresponding Ia fibres. Thus the fibres would be activated prior to or during the experimental condition, which would suppress the H-reflex (Kohn, Floeter et al. 1997).

One obvious solution to prevent this depression would be to reduce unnecessary movement of the limb by securing the relevant joints. However, this is not adequate to prevent changes in isometric contractions. Another suggestion would be to maintain a small, constant contraction in the muscle, which, while itself creating post-activation depression, its effect should be constant between conditions (Misiaszek 2003).

1.5.4   Presynaptic Inhibition

As its name implies, this inhibitory pathway acts via axon to axon synapses between inhibitory interneurons and Ia afferent axon terminals. These connections are known to be GABA-ergic synapses, and the interneurons are labelled PAD (primary afferent depolarization) interneurons (Pierrot-Deseilligny and Mazevet 2000). These interneurons release GABA (gamma aminobutyric acid), which activates corresponding receptors at the Ia afferent terminal, inactivating calcium channels, thereby reducing the release of neurotransmitters (Rudomin and Schmidt 1999). The effects of this pathway are highly dependent on the movement involved, and an example is provided in Figure 1-9, where depression of the soleus H-reflex is observed when Ia volleys are created in the tibialis anterior via vibration (Pierrot-Deseilligny 1997). Results (B in Figure 1-9)
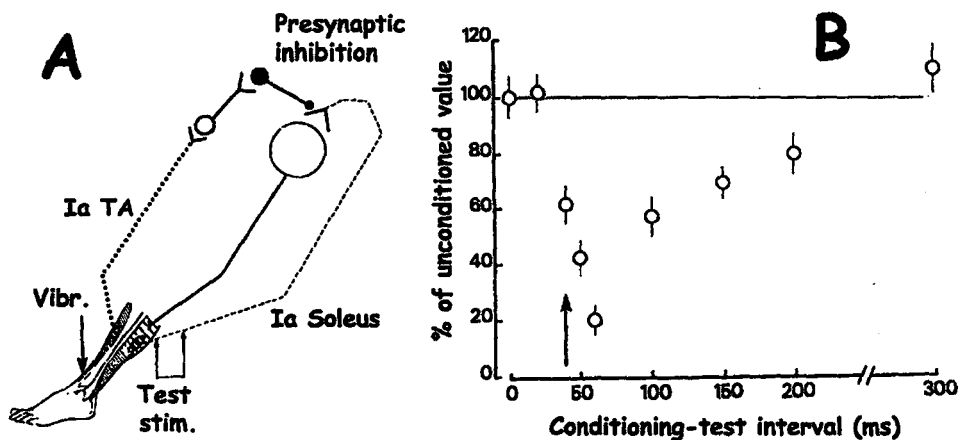

Figure 1-9: Changes in presynaptic inhibition of soleus due to tibialis anterior vibration. In A, open circles represent MNs, and the small solid circle is the PAD interneuron; innervated by the TA MN, and synapse onto the axonal end of the Soleus Ia fibre. In B the results of the amplitude against time of stimulus is shown, indicating an optimal delay when presynaptic inhibition is strongest (Pierrot-Deseilligny 1997).

show that not only is the type of conditioning movement an important influence (in this case a contraction of an antagonistic muscle), but the interval between the conditioning stimulus and the test stimulus (H-reflex on the soleus) is of importance as well, with an interval of about 50ms showing the most inhibition.

Presynaptic inhibition has far reaching effects in that even volleys from distant afferents may cause modulation. For example, passive pedalling motions of the leg, while the ankle remains fixed, causes H-reflex suppression of the soleus H-reflex through this pathway. There is even evidence that this pathway could have effects contralaterally (Cheng, Brooke et al. 1998), as well as a static positioning effect (McIlroy, Collins et al. 1992). The appearance of static and dynamic components to this pathway would seem intuitive as Ia and II afferents also have these two components affecting their firing rate, which here would affect the excitation of the PAD interneurons.

Similar to recurrent inhibition, there also seems to be some amount of descending control of PAD interneurons from the motor cortex. H-reflexes in paralyzed cats were presynaptically inhibited when the relevant brainstem regions were stimulated (Gosgnach, Quevedo et al. 2000). In humans, there is even some evidence showing that mere mental rehearsal or simulation of an action could change the H-reflex response (Bonnet, Decety et al. 1997). The overall effect of this complex system seems to aid in the execution of cortical motor plans, by preferentially allowing Ia afferents to aid in synergistic contractions, while inhibiting the reflex responses from activating irrelevant muscles (Rossi, Decchi et al. 1999).

1.6   Tendon stimulation

As we conclude the background section, some importance must be placed on explaining the various technical considerations and relevant results from various methods of tendon stimulation, as well as review some of the relevant physiological results as they pertain to our current system.

1.6.1 H-reflex work

As seen in the previous sections, the electrically induced H-reflex response is a very popular option for reflexive exploration, likely due to it being an easily quantifiable measure, and the relative simplicity of experimental protocols using standard muscle stimulators. Its main drawback, underlying the methodological ones listed in previous sections, is that H-reflex exploration completely bypasses the muscle spindle itself, as the
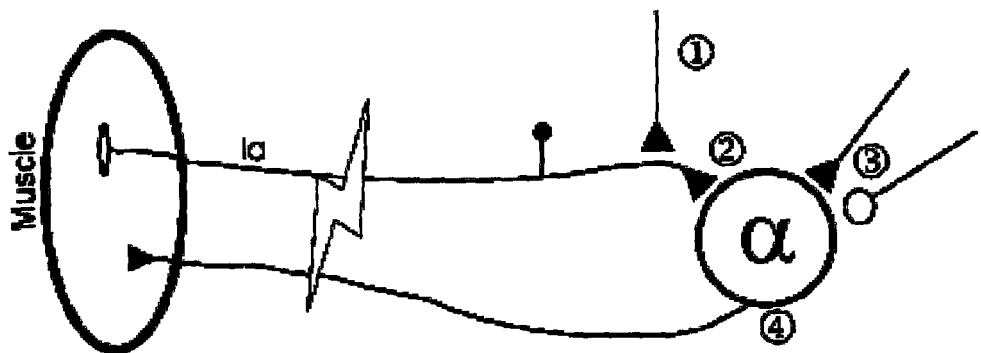

Figure 1-10: The H-reflex response bypassing the muscle spindles (Misiaszek 2003). 1) Presynaptic inhibiting interneurons, 2) Ia afferent axon terminal, 3) Renshaw cells involved in recurrent inhibition, 4) alpha motor neuron.

electrical stimulus replaces the muscle spindles' response up the sensory nerve. This, however, is a poor mimic of a mechanical stimulus, as any pooling, threshold sensitivity or recruitment effects at the spindle level is unaccounted for (Figure 1-10).

The H-reflex is by definition the long latency muscular response to the electrical stimulation of the homonymous nerve. As its use in physiological study has been detailed in the previous sections, we will limit this particular discussion to methodological considerations. Previous work in our lab on the subject used a constant current, manually controlled stimulator, and bipolar electrodes, to deliver electrical pulses to the median nerve at the cubital fossa to excite the FCR (Fu 2005). The main technical considerations here are the pulse shape/duration of the stimulus, the amplitude of the stimulus, and electrode placement/anodal block.

Pulse duration, much as it does in functional muscle stimulation, affects the recruitment of fibres being stimulated; longer pulses recruit more Ia fibres (Burke, Gandevia et al. 1984). Anodal block, where the nerve underneath the anode electrode is hyperpolarized, is an important factor in the placement of bipolar electrodes, since transverse stimulation requires a higher current for most muscles that the H-reflex is used on. Thus the cathode electrode must be placed proximal to the spinal cord (Fu 2005) since the stimulation must be able to travel up the nerve towards the spinal cord. Amplitude of the stimulating pulse is an important measure, as each recording session has highly variable recording and subject conditions. Thus to properly quantify the results the amplitude used must be related to eliciting H-reflex's of a certain percentage of the

maximum H-reflex or M-wave that particular subject was able to elicit that day (Burke,

Gandevia et al. 1984; Delliaux and Jammes 2006).

Other than the clinically standard amplitude based measurements of the H-reflex

(Yablon and Stokic 2004; Voerman, Gregoric et al. 2005), more novel statistics have

been derived, though none have shown significant improvements in reliability or ease of

use over the standard technique (Christie, Lester et al. 2004).

1.6.2   Single tendon tap work

The tendon tap has long been recognized as a mechanical version of the
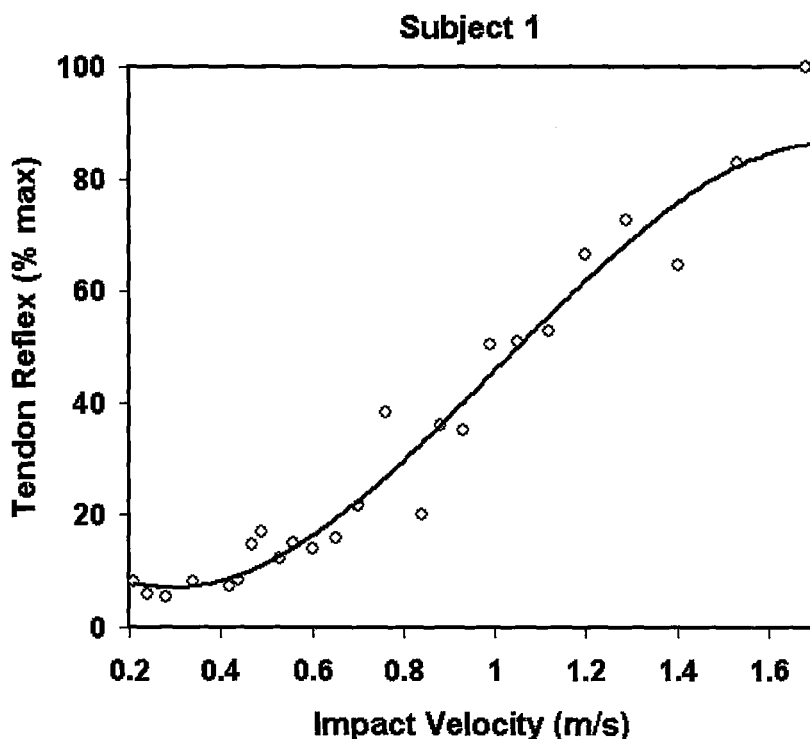
Figure 1-11: FCR response amplitudes to increasing impact velocity

(Archambeault, de Bruin et al. 2006).

electrically induced H-reflex using the same reflex arc, although the afferent volleys are different (Burke, Gandevia et al. 1983). Single tap studies done in our lab have focused on the effects of excursion depth and impact velocity (Figure 1-11) on the amplitude response of the tendon reflex. Results show an initial rise in response as each parameter is increased, with a plateauing, or even a decrease in the case of excursion depth (Figure 1-12), of the tendon response amplitude (Archambeault, de Bruin et al. 2006). As a follow up to these results, the possible contributions of the secondary type II nerve endings is examined as a pilot study with the current system.
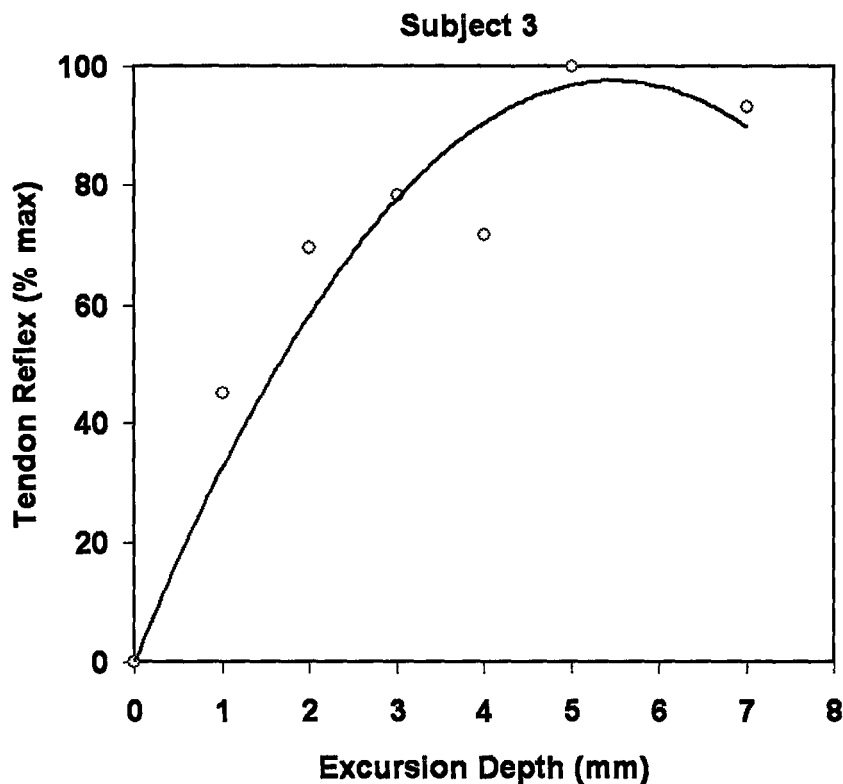
Subject 3

Figure 1-12: FCR response amplitudes to increasing tendon excursion depth (Archambeault, de Bruin et al. 2006).

1.6.3 Vibration work

There has been much work done using vibration to explore human reflexes using vastly different stimulus deliveries, and measurement purpose and methodologies.

Vibration stimuli included purpose built electromagnetic vibrators (Roll, Vedel et al. 1989; Cody, Henley et al. 1998), servo-motors (Albert, Bergenheim et al. 2006; Fallon and Macefield 2007), and standard radial DC motors with eccentric attachments (Nardone and Schieppati 2005; Courtine, De Nunzio et al. 2007). Subject setup was also widely varying, with little to no attention paid to the standardization of subject positioning or stimulation location along the tendon. The actual vibrations delivered by these stimulators during load have only been verified by a small portion of the above mentioned works (Courtine, De Nunzio et al. 2007; Fallon and Macefield 2007).

The bulk of the work done in using vibration to directly explore muscle spindles in normal subjects have been at the microneurographic level (Roll, Vedel et al. 1989; Fallon and Macefield 2007), though some work has been done at the surface level (Cody, Henley et al. 1998). In microneurographic recordings, a micro-needle in inserted through the skin and tissue into the nerve itself, to record the impulses from the neuron directly. The type of neuron being recorded from is then identified by a series of different stimuli (limb movement, muscle contraction, electrical pulses, etc.) that are thought to trigger the isolated firing of the different fibre types (Roll, Vedel et al. 1989). Such experiments employed the use of very low levels of vibration (from 50 to 500 μm), presumably to

avoid recording large alpha motor potentials causing muscular responses, and the possible movement of the needle itself under more violent vibration conditions.

The main results shown in microneurographic work indicate that many muscle spindles, specifically the primary Ia afferent fibres, respond to a wide range of frequencies (up to 200 Hz) and are capable of firing in a 1:1 fashion for almost the entire range (Figure 1-14), with a preferred 1:1 frequency distribution centered around 80Hz (Figure 1-13). Secondary group II endings and Ib endings belonging to Golgi tendon organs exhibit 1:1 firing for a much smaller range of frequencies (below 50 Hz), with most failing to respond at all above 100 Hz (Fallon and Macefield 2007).

Surface recording based work used EMG derived measures, mainly mean signal level and other derivative data such as area under the EMG, as a differentiating statistic (Cody, Henley et al. 1998; Nardone and Schieppati 2005). The power line and vibration noise inherent in these studies cannot be removed by standard frequency domain filtering,
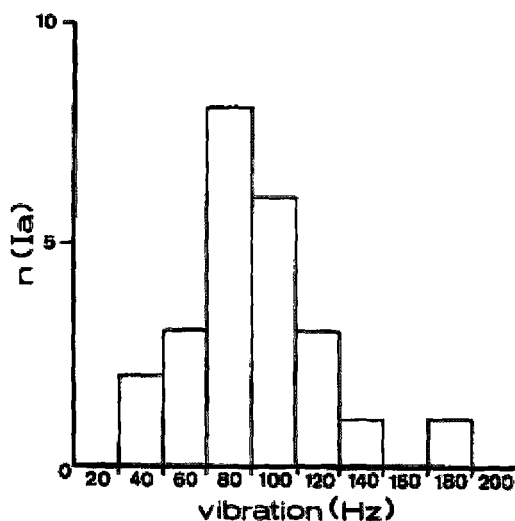
Figure 1-13: Preferred frequency of vibration that caused 1:1 muscle spindle firing (Roll, Vedel et al. 1989).
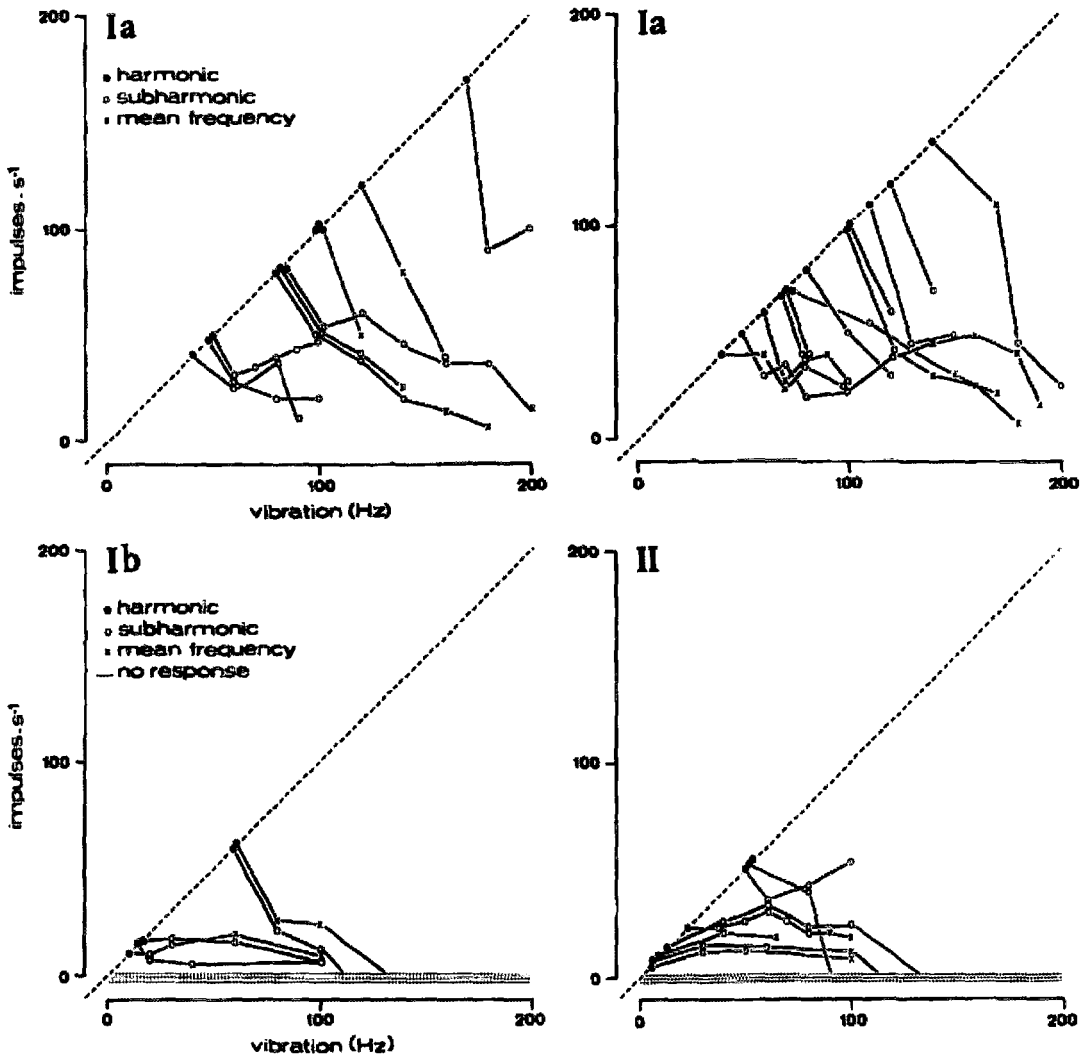
Figure 1-14: Firing responses of Ia (primary), II (secondary), and Ib (Golgi tendon organs) to vibrations up to 200 Hz. Results show that many spindles at the neurological level are capable of 1:1 firing at high frequencies (Roll, Vedel et al. 1989).

since it would likely remove part of the EMG signal as a significant portion of surface recorded EMG spectral energy lie around the 60 Hz frequency. The same applies to vibration noise above 40 Hz, as typical EMG bandwidth is about 40 – 100 Hz.

1.7   Relevance

The above was but a very brief review of the use of the simple reflex arc in studying spinal reflex excitability and its related mechanisms. Although the H-reflex and vibration stretch reflex are simple to use procedurally, much precaution should be taken to reduce, it not eliminate, the effects of the many pathways that are not being studied by an experiment. The stretch tendon reflex's non-invasive nature allows for experiments requiring natural movement and is certainly an invaluable tool in the current day, ethics intensive research environment.

Strictly speaking, as per the original definition (Hoffmann 1952) and already mentioned in 1.6.1, the H-reflex is elicited by electrical stimulation of the motor nerve and is reflective of the activity of the monosynaptic reflex arc. In this project we are also using the term to describe the muscle response to stimulation of the MSs themselves through single taps or vibrations of the muscle tendon. Using this mode of investigation we include the properties of the muscle spindles themselves in our studies.

CHAPTER 2
SYSTEM DEVELOPMENT

2.1   Introduction

This chapter will describe the various parts of this tendon stimulation system, and also present the various developmental challenges, goals, and their solutions, pertaining to this project. Areas such as tendon vibrator control, signal capture and storage, noise removal, post processing and data extraction are described and justified. The general experimental setups used in the pilot studies are presented as well.

2.2   System Description

2.2.1   Overall System

The system, illustrated in Figure 2-1, is centred on the use of a linear motor to deliver tendon stimuli. The motor was previously used to study single tendon taps (Archambeault, de Bruin et al. 2006), and has been reprogrammed to deliver vibration. The system includes a linear motor and its accompanying controller, which is connected to the PC via a standard RS-232 serial connection. On the data capture side, 2 electrodes
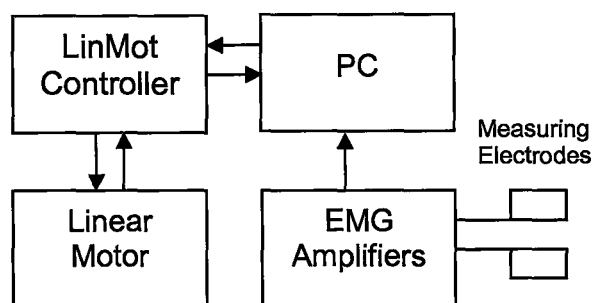

Figure 2-1: Overall system description, a RS-232 serial connection links PC to motor controller; EMG is digitized using an NI 6024E DAQ.

are placed over the muscle of interest and are connected to an A-M Systems instrumentation amplifier. The resultant amplified signal is then digitized using a National Instruments analog to digital converter and recorded by the computer using a custom-written LabVIEW program.

33

2.2.2 Linear Motor

The motor used is a PS01-23x80 motor, paired with a E100 controller, and a S01-48/150 switching power supply, all manufactured by LinMot (Switzerland). This model was chosen for its precision (capable of discrete amplitude increments of 19.53 μm), high continuous force (33 N maximum), almost instantaneous acceleration when unloaded (up to 280 m/s^2), and its low cost. The motor has a 4000 sample memory with which to store motion profile curves; stored in CSV (comma separated value) format files, which are easily manipulated using MATLAB or Microsoft Excel. There are also accurate internal position-tracking capabilities onboard the motor, which are used as a verification of compliance with demanded movements.

2.2.3 Electrodes

Self sticking electrodes were used, made by Tyco Health Care Group (Mansfield, MA). Recording electrodes are 2.2 cm × 1.1 cm, and the grounding electrodes are 2.2 cm × 2.2 cm. These are relatively high impedance electrodes (30 kΩ) and no skin preparation, other than an alcohol swab, was used. These are standard for diagnostic electromyography.

2.2.4 Instrumentation Amplifier

The inexpensive amplifier used was an A-M Systems (Carlsborg, WA), Model 1700, differential AC amplifier. This amplifier is capable of gains from 100-10000, with
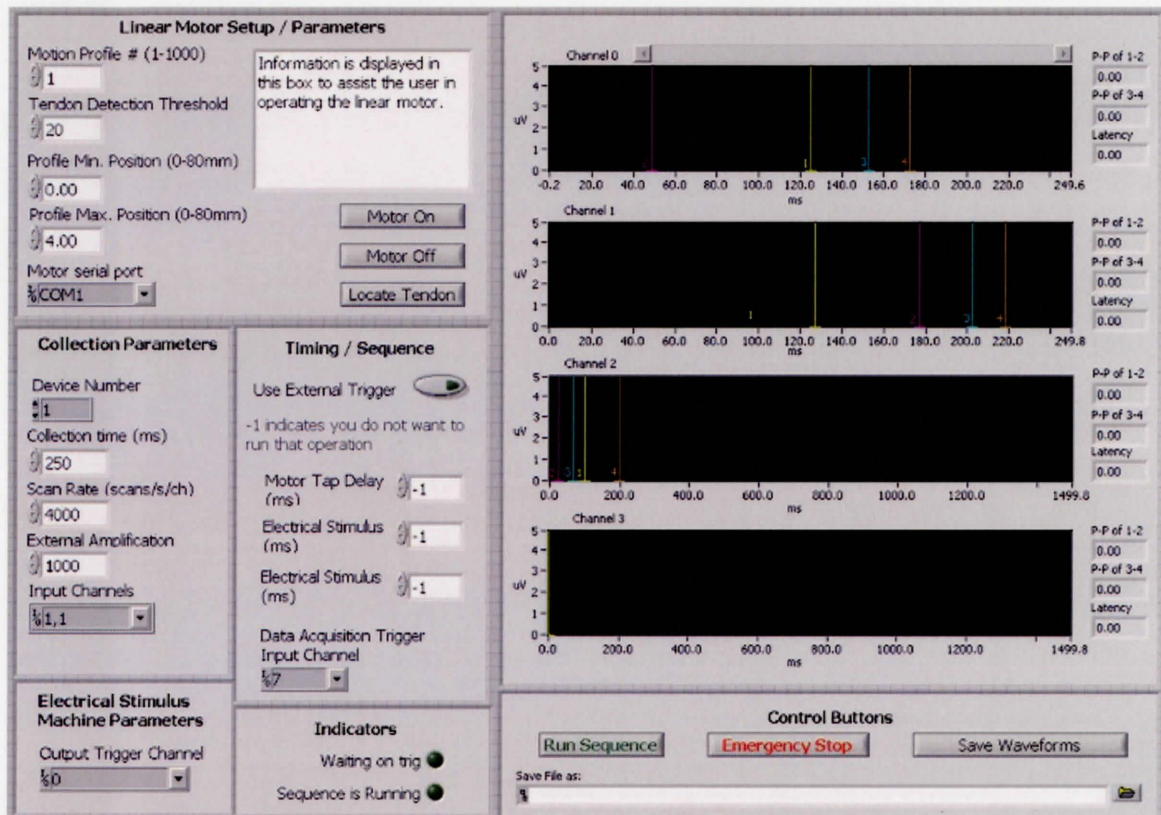
Figure 2-2: Screen capture of the LabVIEW control program, used with all experimental protocols.

a common mode rejection ratio of >70dB at 60Hz. It is connected to the electrodes through the supplied shielded cable.

2.2.5 Computerized Data Capture

The output of the amplifier is digitized using a National Instruments (Austin, TX) PCI-6024E 12 bit internal analog to digital converter card, installed inside a standard Pentium 4 PC. Data capture and storage is done via a custom LabVIEW 8 program, with the interface pictured in Figure 2-2. This program centralizes all of the necessary controls for each of the pilot protocols:

- Linear motor control (selecting which stored motion profile to run, detecting the tendon, and calculating the necessary spatial offsets)

- Collection parameters (sampling rate, collection time, amplification offset)

- Timing (motor tap delay to allow for pre-stimulus recording, external trigger controls)

- Display (typical condensed full signal length display, along with one scrollable expanded display to examine signals in detail without post processing

- Storage (recordings stored in CSV format, easily read by MATLAB post-processing programs, or even Microsoft Excel)

2.3   Motion Planning and System Verification

The first task in the development of this system was to reprogram the motor to deliver sinusoidal vibrations. Therefore, verifying the proper, precise movement of the tendon hammer was necessary to ensure that it delivered the desired actions. Several factors proved to be influential in the movement of the motor, and their effects are detailed in the following sections. That is followed by a description of the finalized motion profiles that were used and possible future improvements in motion planning.

2.3.1   Frequency

The main objective of this tendon stimulator was to deliver sinusoidal vibrations of different frequencies. As such, the first system test performed was to program sinusoidal motions over a wide range of frequencies at a nominal sampling frequency of 1 kHz. Given the motor specifications, it was assumed that the motor could easily follow the trajectories required for relatively low frequency vibrations. However, early H-reflex results were inconsistent with expectations and it was decided to test the motor's compliance with the required trajectories. The results are presented in Figure 2-3 A to E. Note the consistent following of the resultant movement to the demanded frequency. The amplitude and phase, however, are more and more in error as frequency is increased. Resultant amplitude was especially unpredictable, decreasing from 5-15 Hz, but increased for 15-30 Hz. Phase shift increased consistently, though that is to be expected as a result of the motor having to overcome its own inertia for such small but rapid movements.
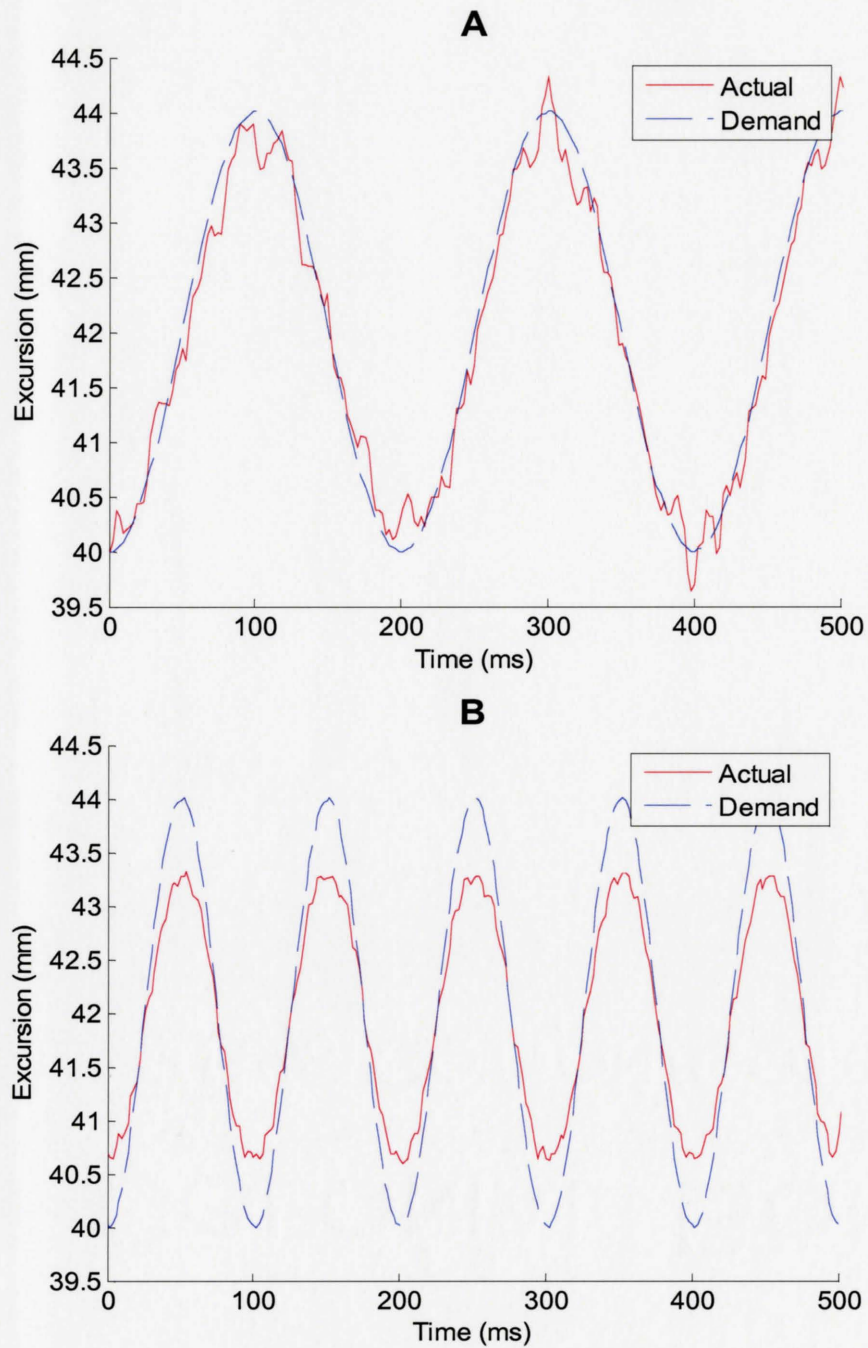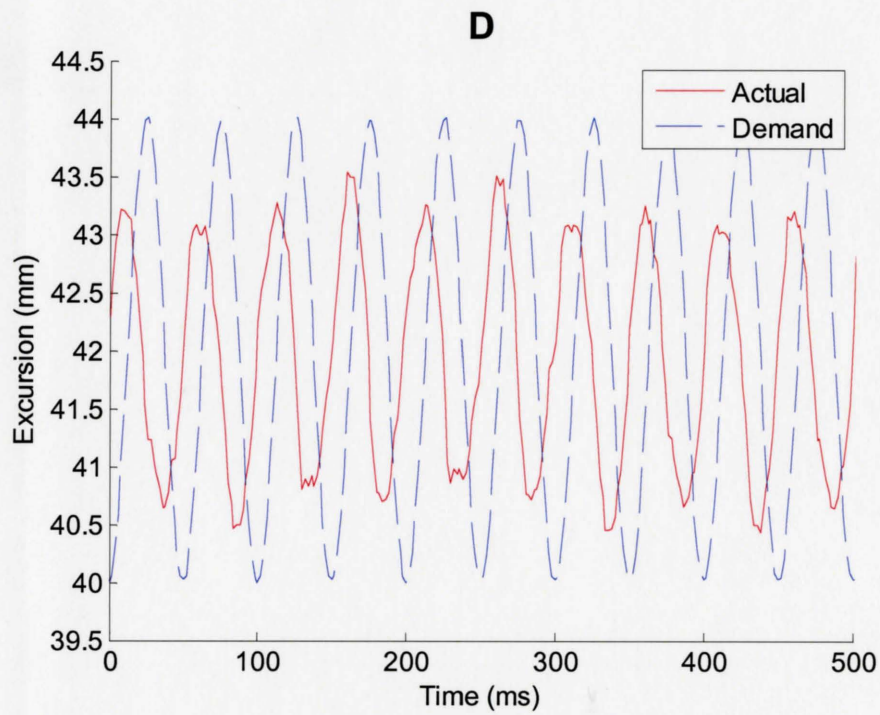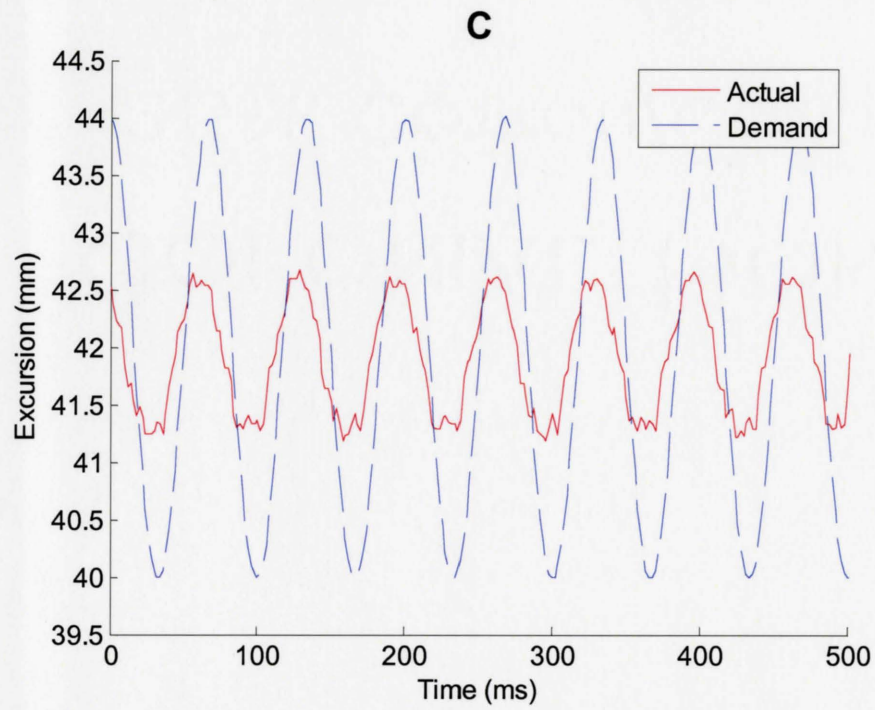
Figure 2-3: continued on next page.

C
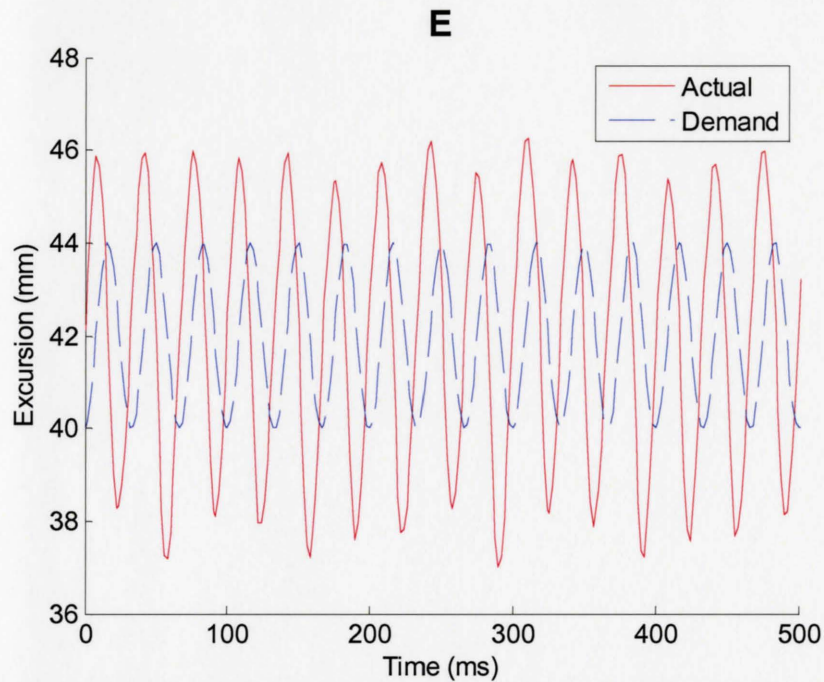

D

Figure 2-3: continued on next page.

Figure 2-3: Demand vs. actual movement for 1 kHz sampled sinusoids of different frequencies (A – 5 Hz, B - 10Hz, C - 15 Hz, D - 20Hz, and E - 30Hz). The demand curve in E appears jagged due to the limited sample memory in the motor's position tracking component.

2.3.2   Sampling Rate

The initial reaction to the above problem with increasing frequency was to increase the sampling rate of the demand sinusoid, thinking that the high frequency profiles were under-sampled. This led to an unexpected effect, illustrated using 5 Hz in Figure 2-4 and 30 Hz in Figure 2-5.
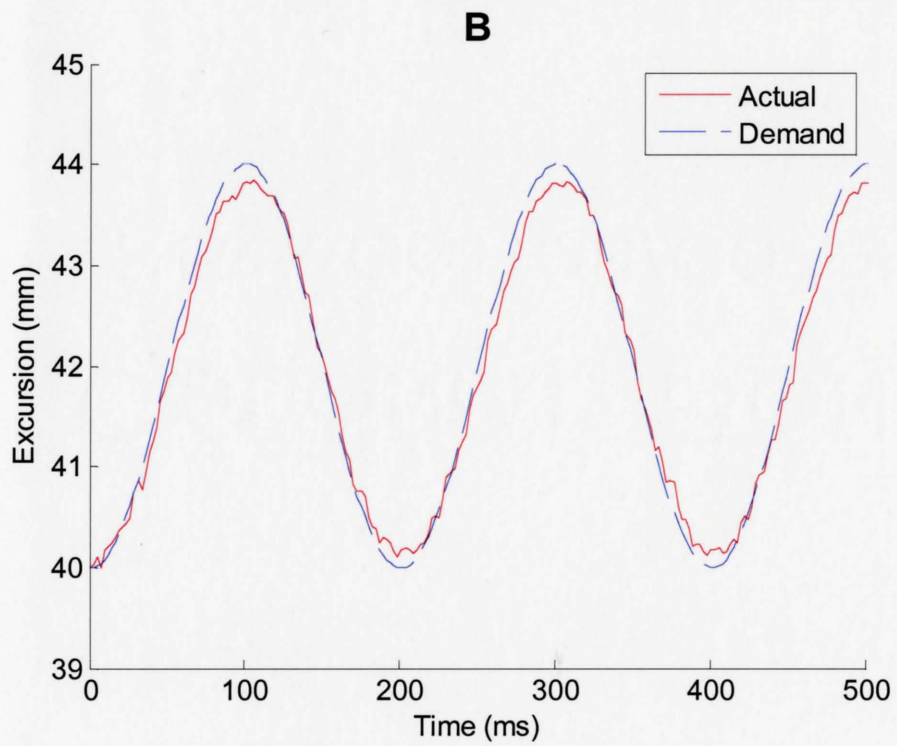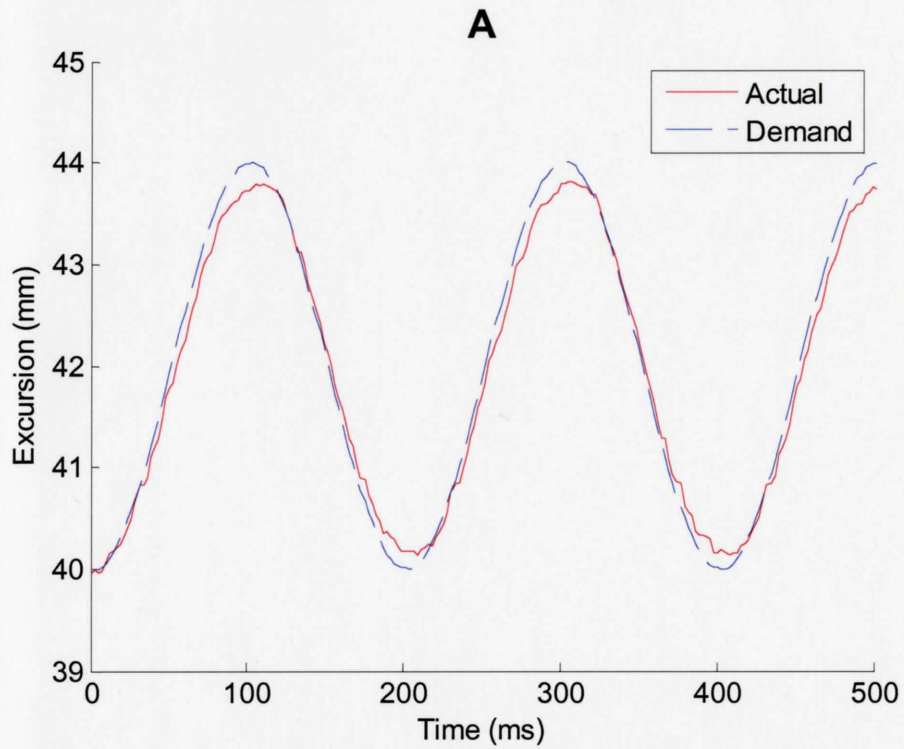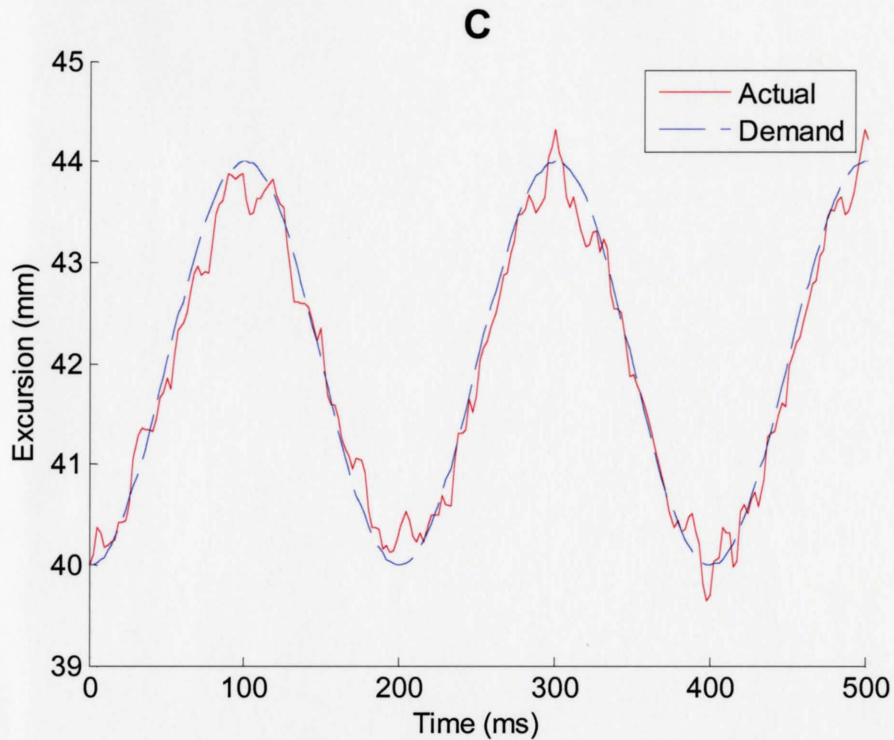
Figure 2-4: continued on next page.

Figure 2-4: A 5Hz vibration profile for different sampling rates (A - 0.25 kHz, B - 0.5 kHz, C – 1 kHz). Note the increased jitter at 1 kHz.

Motion jitter is introduced as sampling frequency is increased. This effect is amplified for higher vibration frequencies, shown in Figure 2-5, as the jitter begins to dominate the resultant amplitude, causing completely erratic amplitudes. It is possible that at higher sampling rates the motor and its control feedback mechanisms are unable to keep up with the volume of instructions fed to it, and therefore demonstrate some sort of delayed reaction or failed to react to certain samples at all, resulting in the jitter.
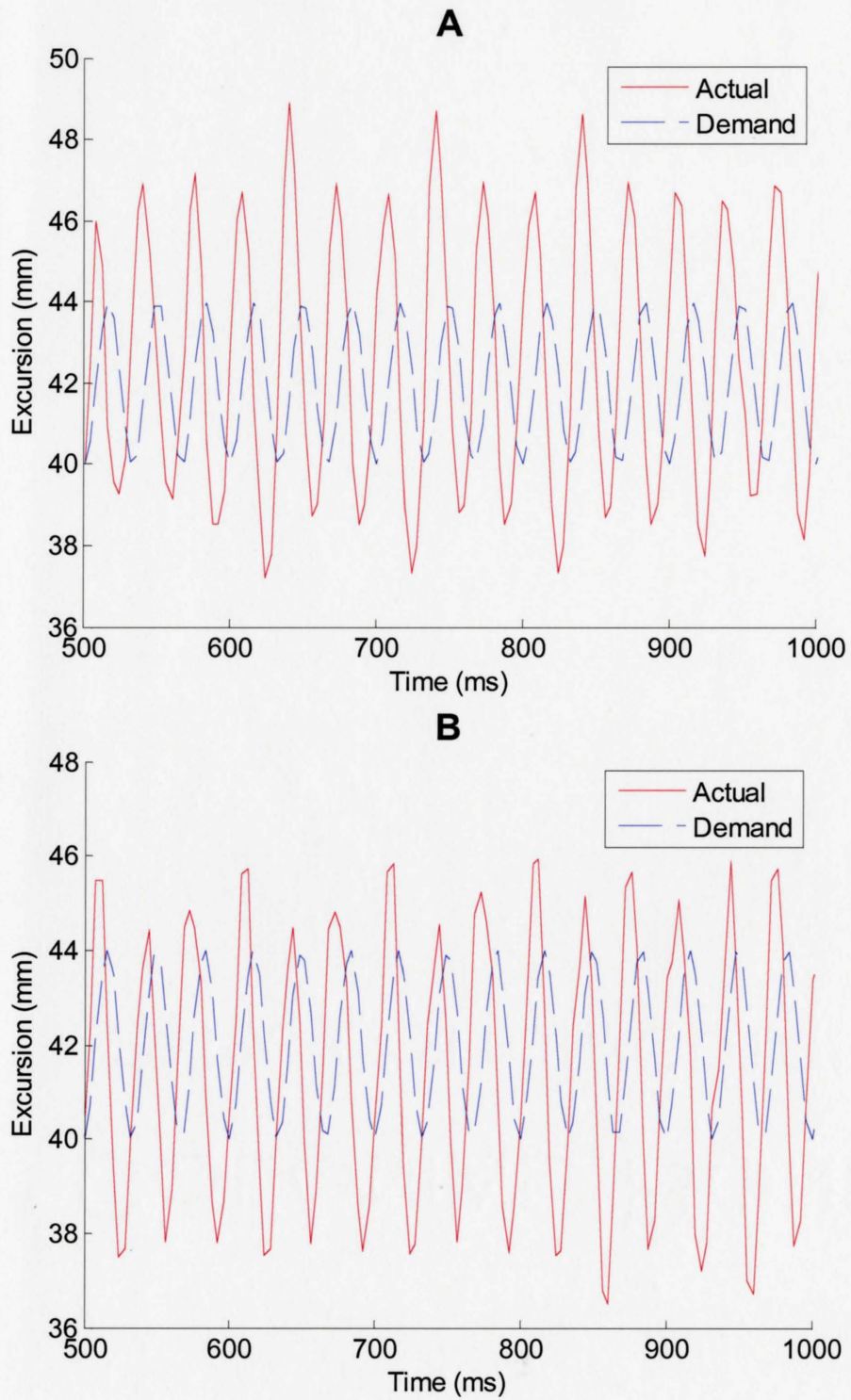
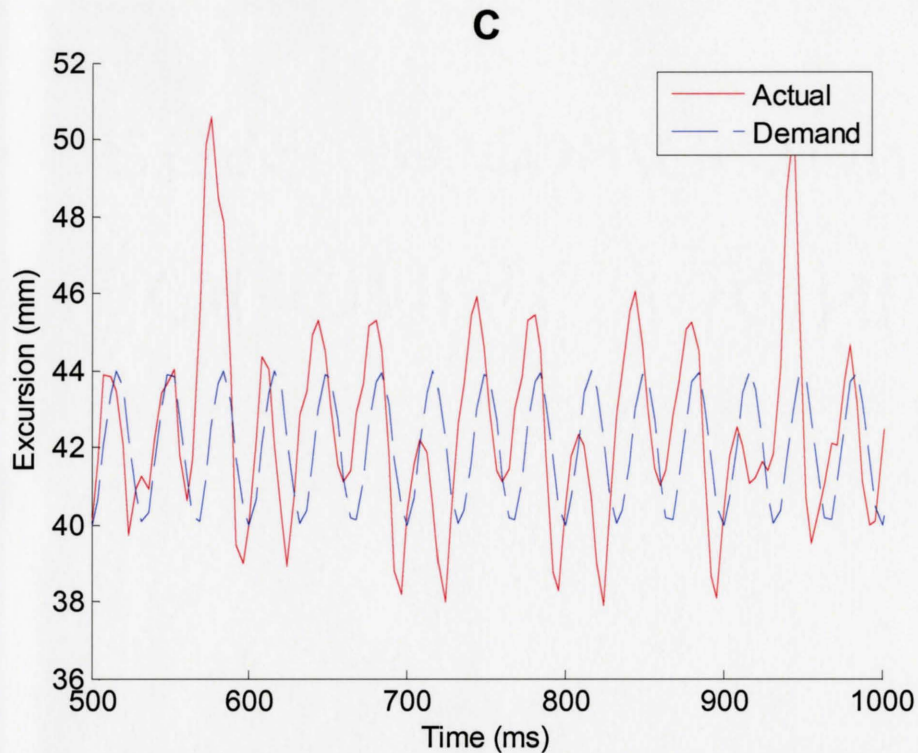**Figure 2-5: continued on next page.**

Figure 2-5: 30Hz vibration profiles for A - 1 kHz, B -1.5 kHz, and C -2 kHz sampling rates.

2.3.3   Finalized Motion Profiles

We concluded that strict sinusoidal motion profiles could not be used for high frequency vibrations with this motor. Upon exploring profiles of other wave shapes, it was shown that square wave profiles resulted in a pseudo-sinusoidal behaviour at higher vibration frequencies. The results are shown in Figure 2-6.
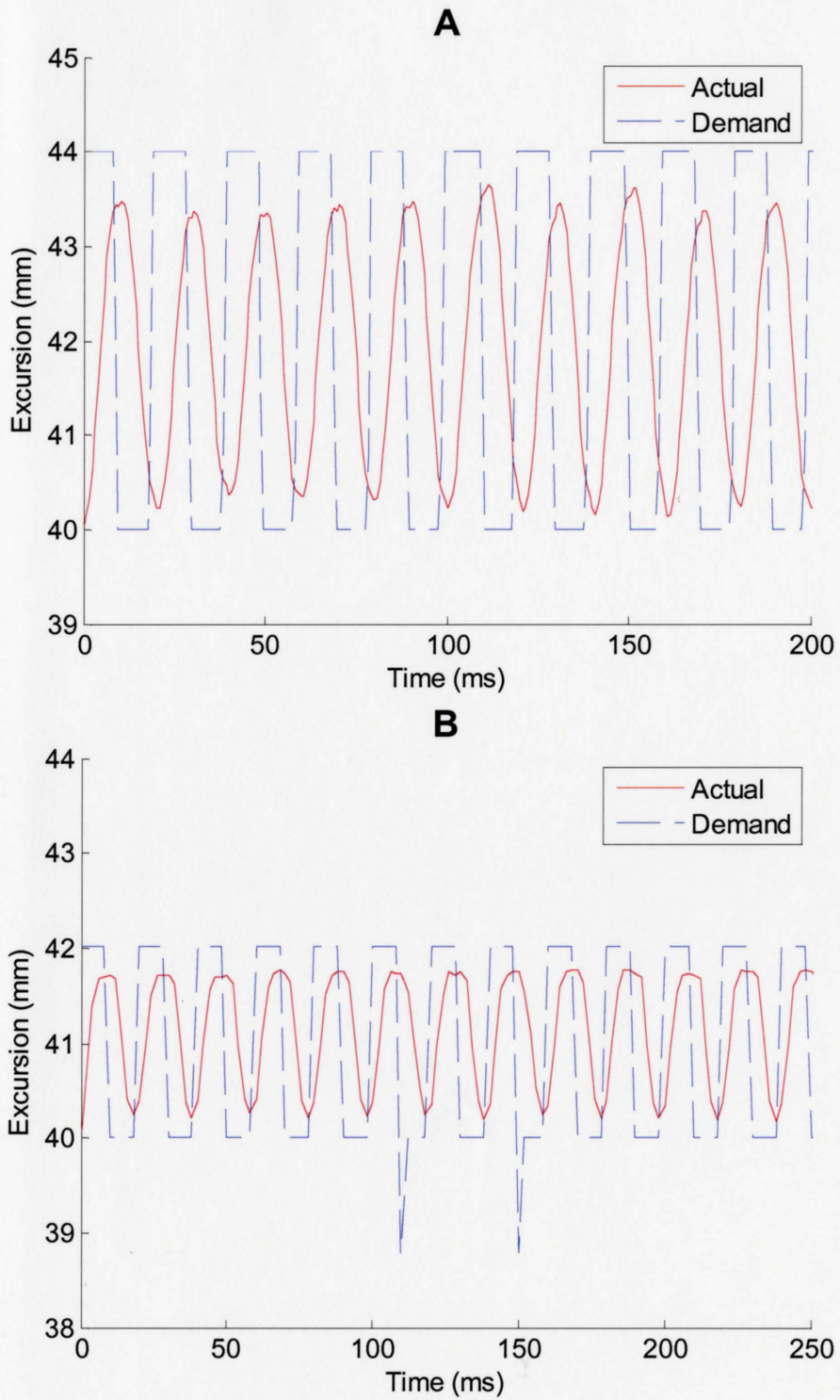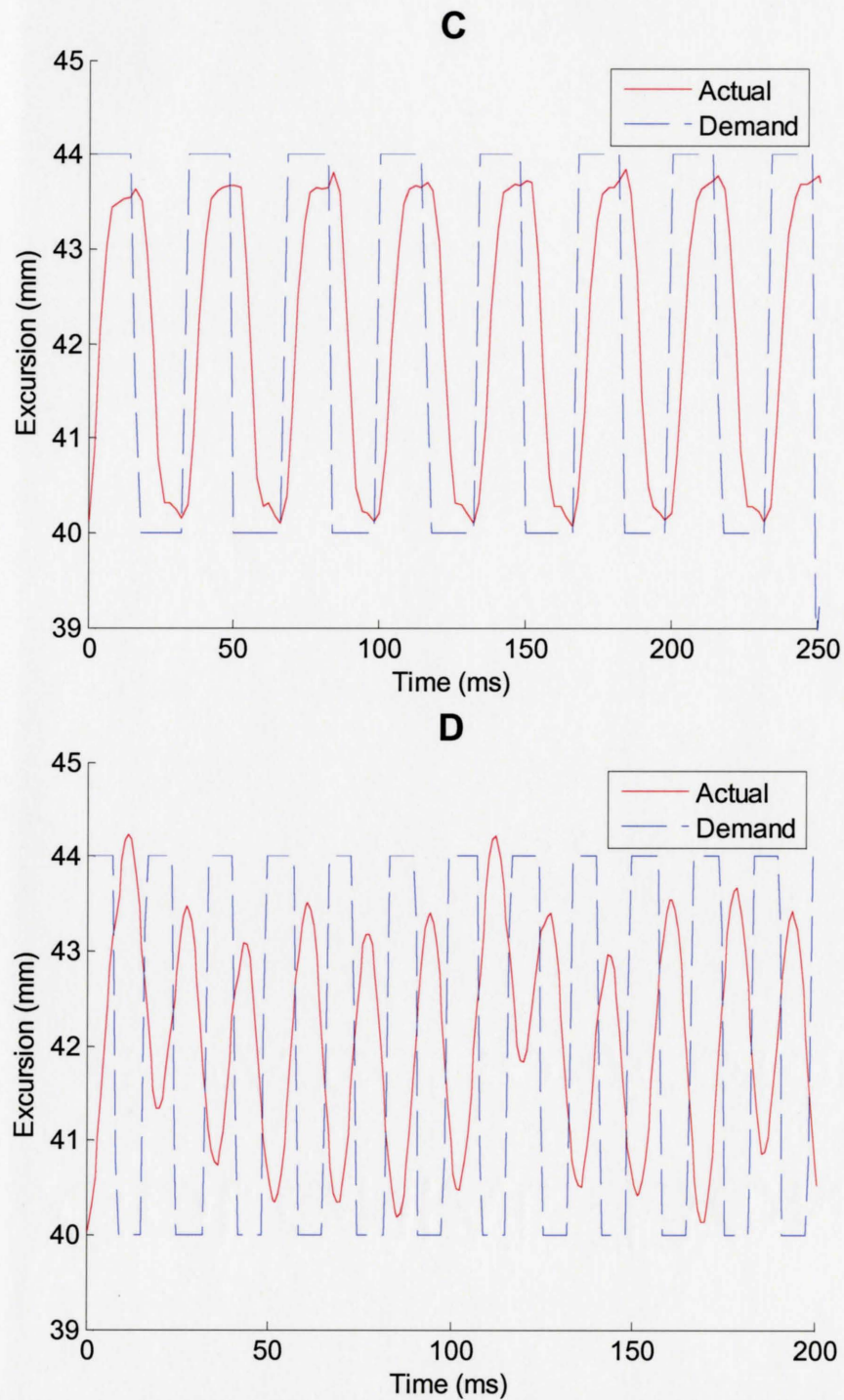
Figure 2-6: continued on next page.

Figure 2-6: Results of using square wave profiles. A - 4mm, 50Hz, B - 2mm, 50Hz, C - 4mm, 30Hz, D - 4mm, 60Hz.

The pseudo-sinusoidal behaviour is much more predictable, even for higher frequencies, than strict sinusoids. It also scales to different excursions and sampling rates consistently. The frequency limit appears at 60 Hz, when motor excursion is no longer consistent, and variability exceeds 1 mm. One favourable side effect is that square waves require much fewer samples to properly define than sinusoids, thus more profiles can be stored simultaneously in the 4 kb sample memory of the motor. This is useful because certain experimental protocols call for multiple profiles, and delays between trials must be reduced to minimize temporal biological variability.

After these system tests, the decision was made to use strict sinusoids for frequencies less than 15 Hz, and square waves for anything above that, up to 50 Hz. An area of interest for further work could be the 12-17 Hz range, where the vibration frequency is too high for a strict sinusoid but too low for the square wave to produce a reasonably sinusoidal result. A trapezoidal motion profile could possibly be used as a bridge between square and sinusoidal profiles at these cross-over frequencies.

CHAPTER 3
PHYSIOLOGICAL TESTS

3.1   Introduction

The new tendon analysis system was tested using two male subjects, age 63 and 25 respectively. The study was approved by the research ethics board of Hamilton Health Sciences. The objectives of the tests were to determine (i) whether H-reflexes could be elicited using larger amplitude vibrations than those in sub-threshold studies; (ii) whether the amplitude and timing of the H-reflexes could be measured more accurately than that reported by Cody, Henley et al. (1998) and Nardone and Schieppati (2005); (iii) whether the H-reflexes were entrained with the stimulus over a range of vibration frequencies; (iv) whether the H-reflexes elicited using this method were affected by low levels of agonist or antagonist contractions similar to Pierrot-Deseilligny (1997) and Fu, de Bruin et al. (2004); (v) whether a separation of the Ia and Ib pathways could be detected as separate spike responses at low vibration frequencies.

The results of (i) and (ii), along with the basic subject setup used in each of the above pilot studies, are presented in this chapter.

3.2   Subject Setup

All experiments were performed on the Flexor Carpi Radialis (FCR), the pronator of the forearm. At the beginning of each experiment each subject was seated in front of the apparatus, shown in Figure 3-1. The chair was adjusted for proper height to ensure a relaxed arm, and a slightly flexed (120 deg) elbow, when placed under the linear motor. The subject's arm is further supported below by bean bags for stability and to reduce vibration movement of the electrodes during the experiment.

The electrode placement on the FCR was found via palpation upon isometric pronation of the forearm. The recording electrode sites, placed 2.5 cm apart over the main muscle belly, were slightly abraded and cleaned using alcohol wipes. The grounding
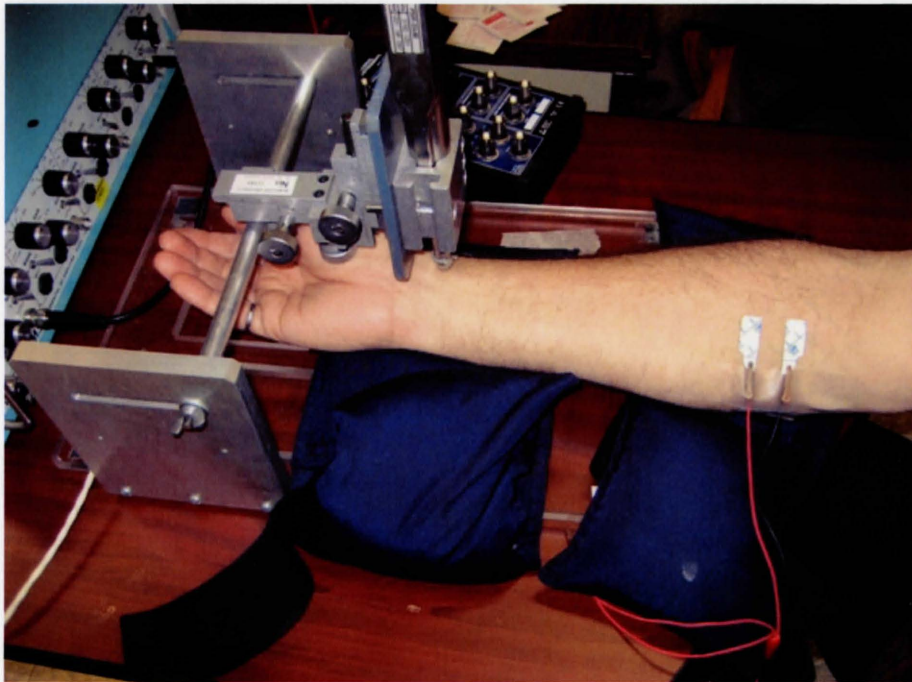

Figure 3-1: Experimental apparatus and setup for a right forearm.

50

electrode was placed on the forearm beside the medial epicondyle. They are connected to the amplifier using its supplied cable, tipped by alligator clips.

The linear motor was positioned, using the micro-manipulators on the mounting rig, such that it was directly over the tendon connecting the palm to the FCR, 4cm proximal from the skin crease that separates forearm from hand. The LabVIEW software will then detect the location of the tendon by slowly extending the motor shaft until it presses on the tendon and a certain resistance is reached. The software will then position the hammer on the skin over the tendon, to minimize the travel time necessary to reach the tendon. The motor shaft could be further lowered or raised a small amount when necessary to avoid the effects of skin and tissue compression. Thus the vibration profiles are only responsible for the vibration motion and not the motion of the motor to make contact with the tendon.

3.3   Data capture, noise reduction, and post processing

The LabVIEW software, running on a standard Windows-based PC, along with the A-M Systems differential AC amplifier and a National Instruments analog to digital converter, sampling at 4 kHz, recorded the electromyographic data. The resultant signals
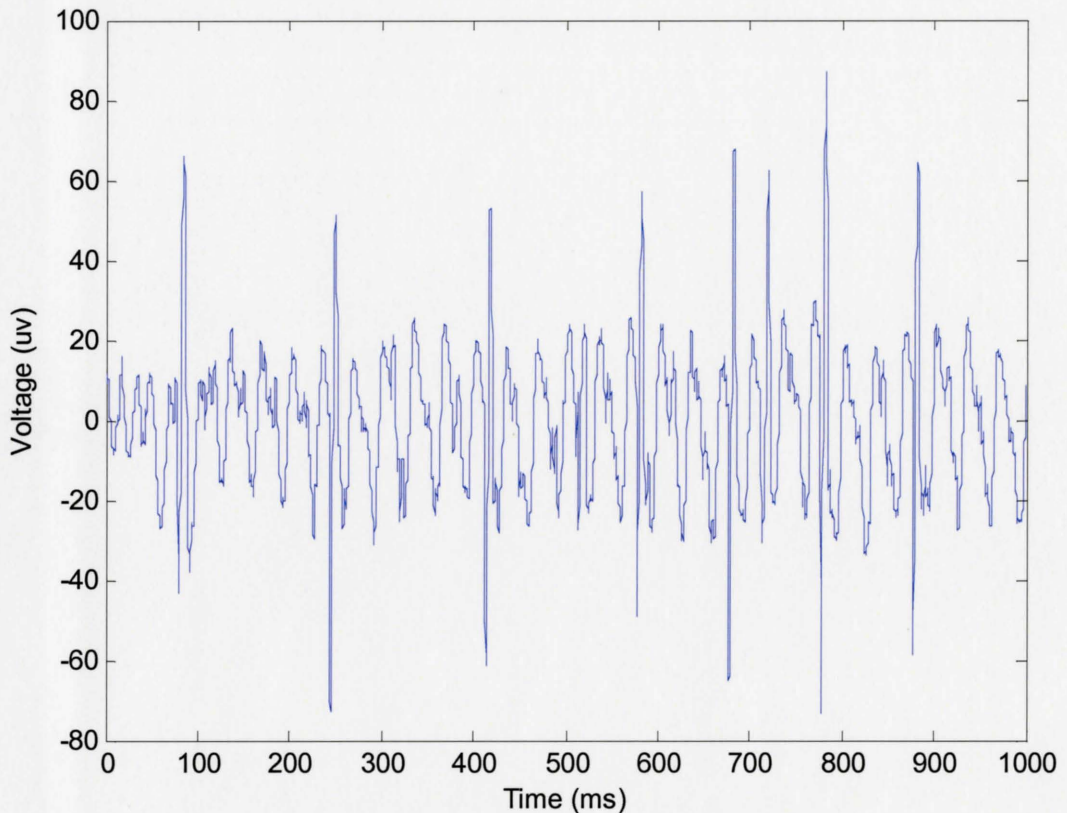
Figure 3-2: Unprocessed recording for a 30Hz, 1s vibration.

were amplified by 10000, hardware band-pass filtered from 10 to 500 Hz (both done by the amplifier), and subsequently stored in comma-separated value (CSV) format files. All post processing was done using MATLAB 7.1. Figure 3-2 shows a raw, unfiltered recording, before any processing was done in MATLAB. Note the large amplitude,

periodic noise, which may have possibly obscured a response spike at around the 500ms mark.

As already seen in Figure 3-2 and again in Figure 3-3 the dominant noise sources in the recorded signal seem to be 60 Hz and vibration frequency motion artifact. Figure 3-3 is a noise recording obtained with a 4 mm vibration of the tissue just lateral to the muscle tendon. The excessive 60 Hz noise is due to the high electrode impedance and proximity to the amplifiers, motor drives, and computers. The laboratory did not allow
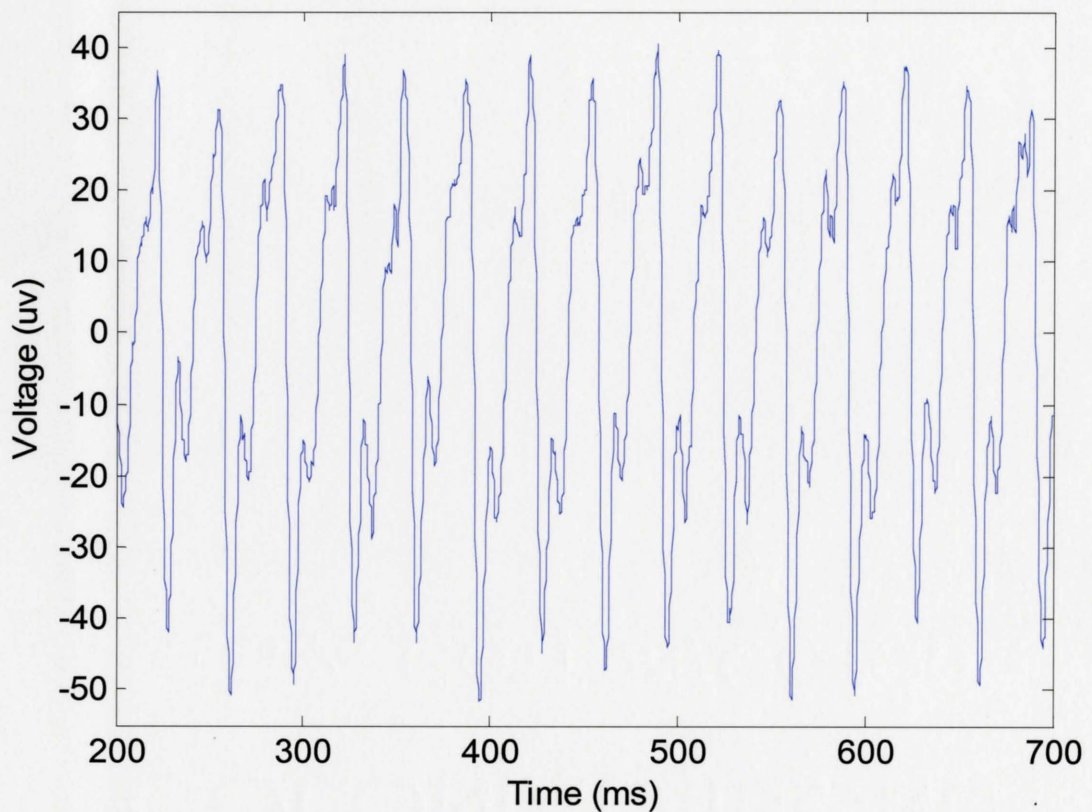

Figure 3-3: 30 Hz vibration noise recorded from vibrating the tissue next to the tendon.

placing the subject distant from these noise sources. Frequency domain filtering, whether using a 60 Hz notch filter or a high pass motion artifact filter, would cause distortion of the evoked M-waves. Consequently coherence dependent, subtractive filters, shown in Figure 3-4, were used to remove power line and motion artifact noise from both single tap, and vibration recordings.

The subtractive filter detects the amplitude and phase of the coherent 60 Hz power noise signal from post-stimulus or pre-stimulus data, and generates a matching 60
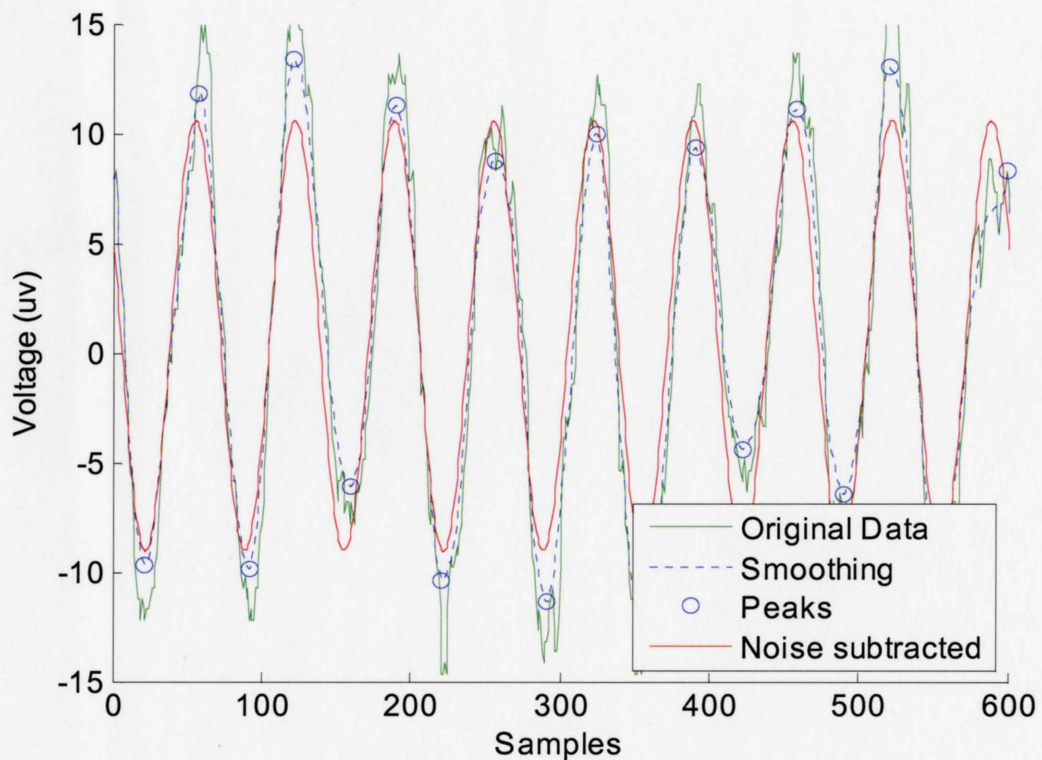
Figure 3-4: Successive steps of the subtractive filter for a post-stimulus recording of 60Hz power-line noise.

Hz sinusoid, which is then subtracted from the signal. The steps in detail are as follows:

1. The original signal is smoothed by a median filter, with a window size that is relative to the sampling rate (in this case, for a 4 kHz sampling rate, a window size of 9 samples was used). This was done to remove high frequency instrumentation noise.

2. The peaks and troughs of the signal were found by first rectifying the signal, and then successively finding the maximum of the signal, then reducing the amplitude of the current maximum and its surrounding samples to 0. The locations and amplitudes of the peaks are stored.

3. A sinusoidal signal is generated. Its amplitude being the average amplitude of the peaks and its frequency set to 60 Hz for power noise, or the vibration frequency for motion artifact noise.

4. The optimal phase of the generated noise signal is determined by successively lining up the noise signal with a peak location, subtracting the noise signal from the original signal, and calculating the FFT of the result. The peak location that results in the lowest 60 Hz or vibration frequency peak in the resultant FFT is chosen as the optimal phase.

This filter significantly reduces the 60 Hz noise power, while preserving the time-domain characteristics of the responses in question. Similarly, a vibration noise sinusoid can also be constructed for each recording since its frequency and phase is locked to the

vibration waveform. Comparisons between this type of filtering and typical frequency domain based digital filters, especially high-pass filters normally used to remove low frequency motion noise, show that subtractive filtering preserves signal shape. This is of importance when attempting to identify the latencies and duration of such responses.

Figure 3-5 shows the same unfiltered response recording to a 30 Hz, 1s vibration as Figure 3-2, along with the filtered version on the bottom. Their power spectrums are shown in Figure 3-6. Through this time domain filter, response spikes that were obscured by noise are now clearly visible, and are easily detectable through simple techniques such as amplitude thresholding. There is some residual noise because neither the vibration nor 60 Hz noise can be completely identified.

In addition to post-processing techniques, simple steps were taken to minimize how much noise we record to begin with. To reduce the 60 Hz contribution, we grounded the entire hammer apparatus to the ground of the amplifier. We also moved the entire experimental setup onto its own table as far away from the recording computer as possible, the power supply of which was radiating 60 Hz. For vibration noise, we used the bean bags as mentioned in 3.2. For certain frequencies that generated more violent apparatus shaking (possibly due to mechanical resonance), gentle pressure over the recording electrodes by the tester's fingers reduced the vibration noise.
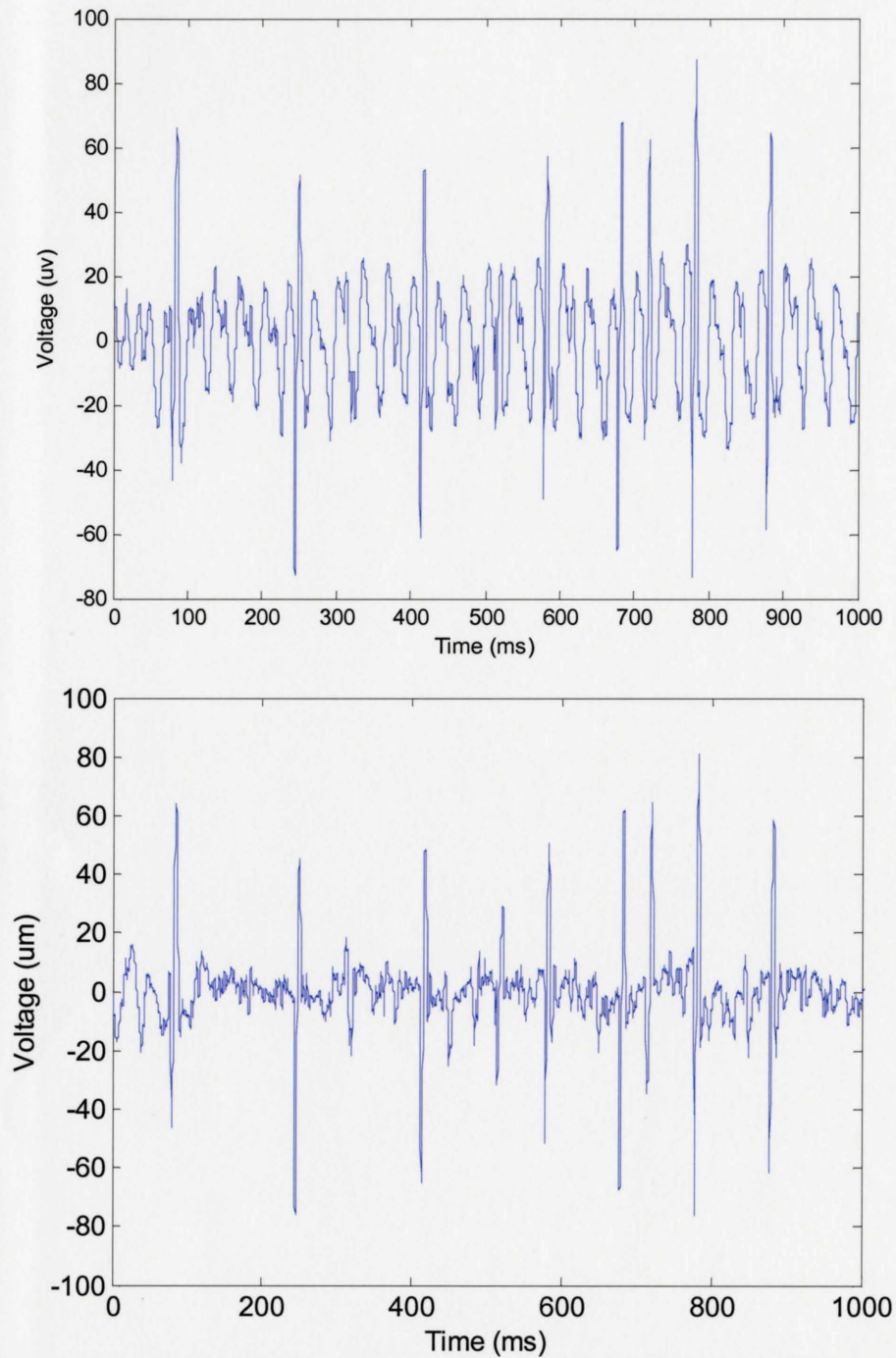
Figure 3-5: Response recording for a 30Hz, 1s, 4mm vibration, unfiltered on the top, filtered on the bottom. Note the presence of an additional response around 500ms that is now visible because of the filtering.
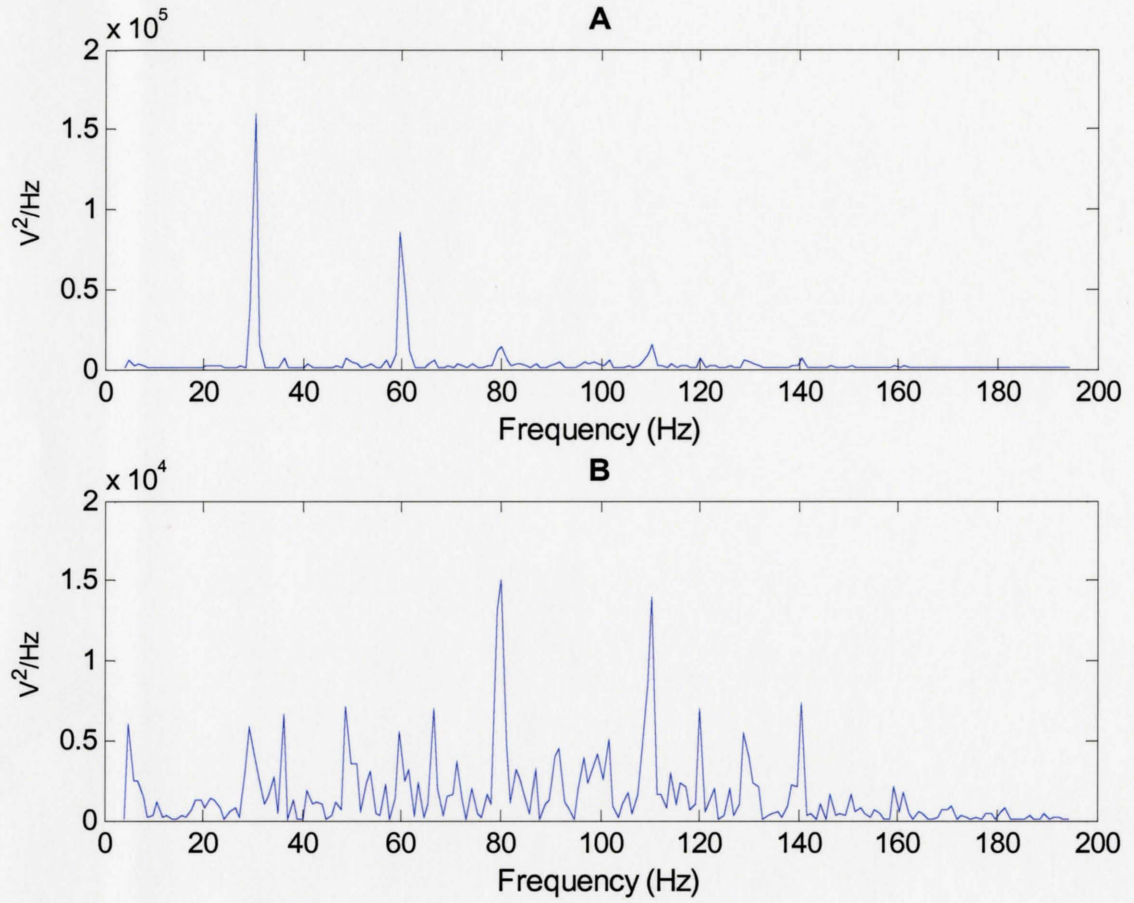
Figure 3-6: Comparison of power spectrums before and after filtering for Figure 3-5. A – before filtering, B – after filtering.

3.4 Data Extraction

The main variables to be extracted from the filtered waveforms are the latencies and amplitudes of the H-reflex or stretch reflex response spikes. As mentioned in the previous section, simple peak-to-peak thresholding was used to detect the spikes. The response trains at the frequencies currently being tested are phase locked to the fundamental vibration frequency, or otherwise are sub-harmonics of it. Therefore, each recording was divided into time segments, the length of which is determined by the vibration frequency (as it is the highest frequency at which spikes will appear). The software can also use windows of different sizes, as illustrated in Figure 3-7, where the portions of signal between the windows are ignored. This is especially useful for low frequency vibrations where there is significant time between stimuli to show background EMG noise. This is illustrated in Figure 3-7, where fifteen 30 ms windows are placed onto a 15 Hz, 1 s vibration recording, with the time between each segment ignored. In detail:

1. The software first detects the time of occurrence of the first response spike within the first 100ms, determined as the first maximum above threshold that occurs within the first 100ms. This is to account for the delay in recorded response due to the finite conduction velocity of the induced Ia afferent signal up the arm and through the spinal cord, and the subsequent activation and travel of the motor unit action potential to elicit the reflex.
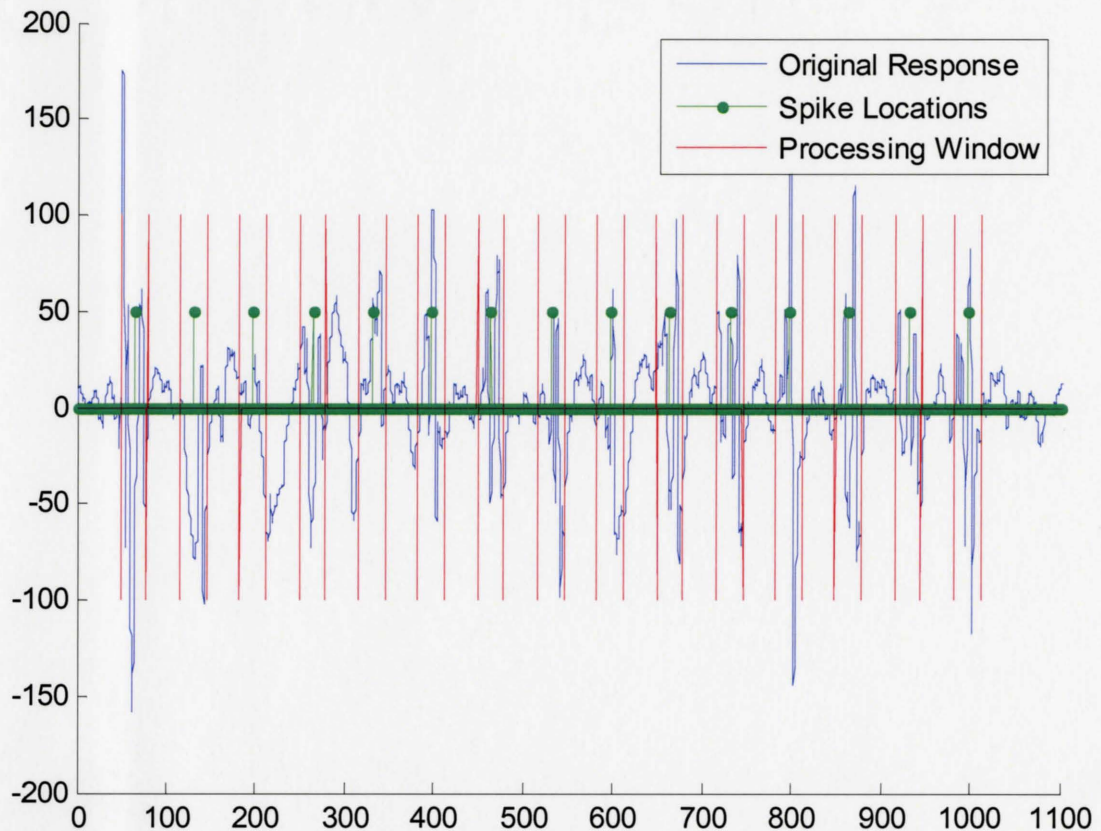
Figure 3-7: Segmentation of filtered signal for data extraction.

2. Subsequent response spike locations are estimated as integer multiples of the vibration frequency period, shown as the solid circles in the figure.

3. The boundary of each window is determined by the manually set window length, each centred on the estimated response locations. This is shown as the vertical lines flanking each solid circle.

4. Thresholding, response amplitude, and time of occurrence are all calculated within these windows.

The threshold is determined visually for each recording, though it tends to be consistent in multiple recordings of the same protocol for the same subject and recording day. The calculations for peak-to-peak response amplitudes, and specific time of occurrence of the response spike, are done within each window. Specifically, the time of occurrence of each spike is determined as the mid point between the time of maximum amplitude within the processing window, and the time of minimum amplitude. The peak-to-peak amplitude is the difference between the maximum and minimum amplitudes within the segment. Any windows whose maximum peak-to-peak amplitudes are below threshold are ignored. These results are also verified visually to detect any anomalies, such as large, movement-induced motion artifacts.

CHAPTER 4
RESULTS

4.1 Introduction

As mentioned in 2.1, this system was used in several pilot studies of the monosynaptic spinal reflex. Already stated previously, 2 male subjects were used in these pilot studies; subject one being 25 years of age, and subject two being 63 years of age, both right handed. All data shown are from the subject's dominant arm.

The results of these studies are presented in this chapter. Specifically, we wanted to investigate the following questions:

1. Would the recorded reflex responses be entrained to the stimulus over a range of vibration frequencies? As mentioned in 1.6.3, individual muscle spindles are able to fire at high frequencies, up to 200 Hz in some cases. Yet significant spinal inhibition prevent the H-reflex from being elicited at rates over 0.2-0.3 Hz (mentioned in 1.5.3). As surface recorded, vibration studies are a bridge between the two methods, would the same limit be observed in stretch reflex recordings? How does the degree of response entrainment change with vibration frequency?

2. As discussed in 1.5.4, presynaptic inhibition excites or inhibits the electrical H-reflex depending on agonist or antagonist activity. Could such effects be observed when similar stimuli are replicated using tendon vibration? Are its effects mainly amplitude based, or does it also affect the degree of response entrainment?

3. As mentioned, Ia (primary) afferent fibres respond more to changes in the rate of change in muscle length, whereas II (secondary) fibres respond to slower changes, or the static stretch, in muscle length. Since these fibres have vastly different diameters (the Ia axons are typically double the size of the II axons), and thus different conduction velocities, would we observe separable responses elicited from each ending at some low cross-over vibration frequency?

4.2   *Entrainment of response train to stimulus*

The degree of entrainment (in percent) is defined as the number of identified reflex response spikes divided by the number of individual stimuli in the vibration train (e.g. 30 for a 1s, 30 Hz vibration) x 100. Figure 4-1 illustrates this concept with a recording that has a 100% degree of entrainment:
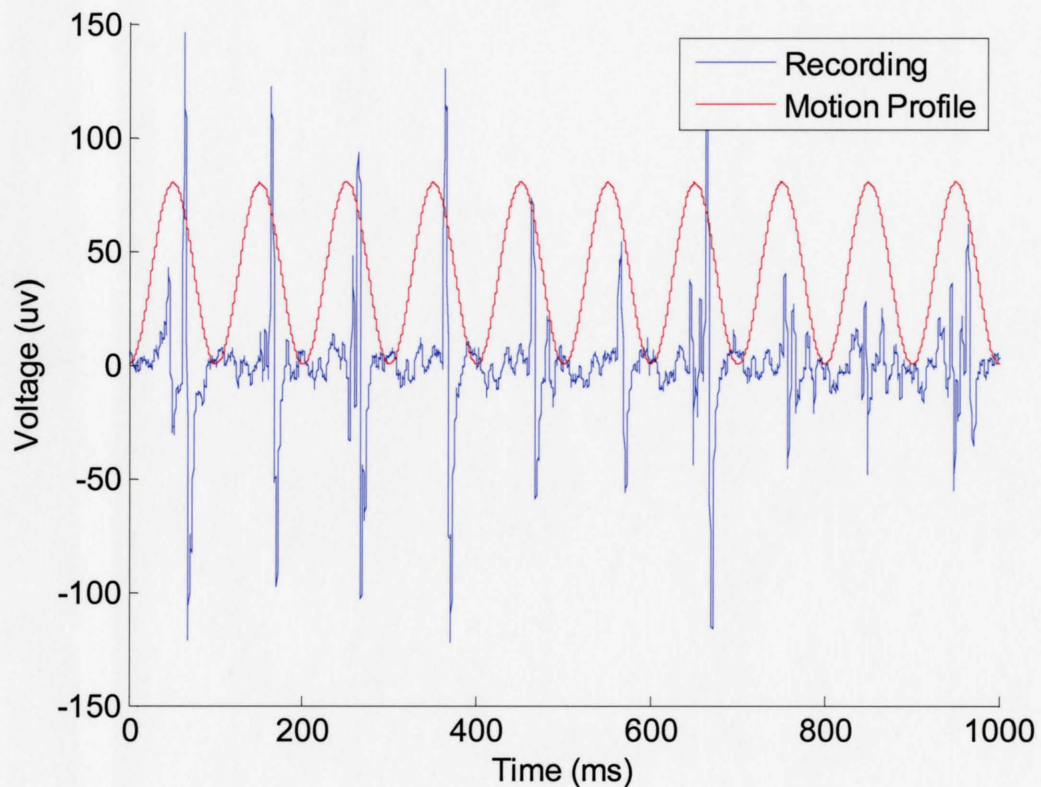

Figure 4-1: Recording of subject 1's response to a 4mm, 1s, 10 Hz vibration. The sinusoid overlaid is the vibration profile. Note the entrainment of the response to the vibration and the consistent phase delay throughout (though the delay is not a factor in our entrainment calculations).

Responses for 4mm, 1s, vibrations at 10, 15, 20, 15, and 30 Hz were recorded for each subject, with 5-6 trials per frequency. The response spikes in each recording were identified and counted, and the degree of entrainment then calculated. Typical recordings of this protocol for subject 1 (for 10, 20, and 30 Hz) are shown in Figure 4-2, and subject 2's results are shown in Figure 4-3.
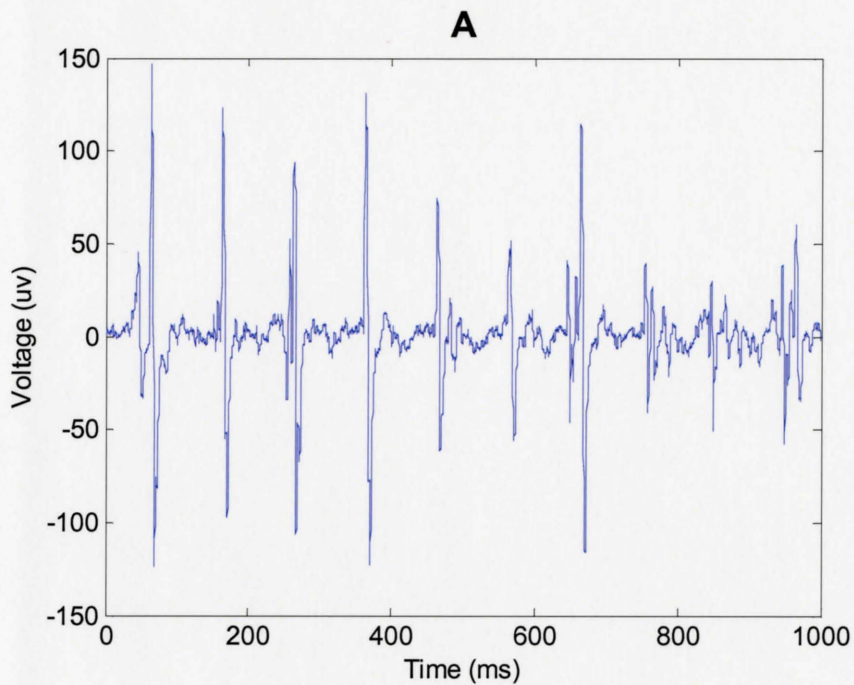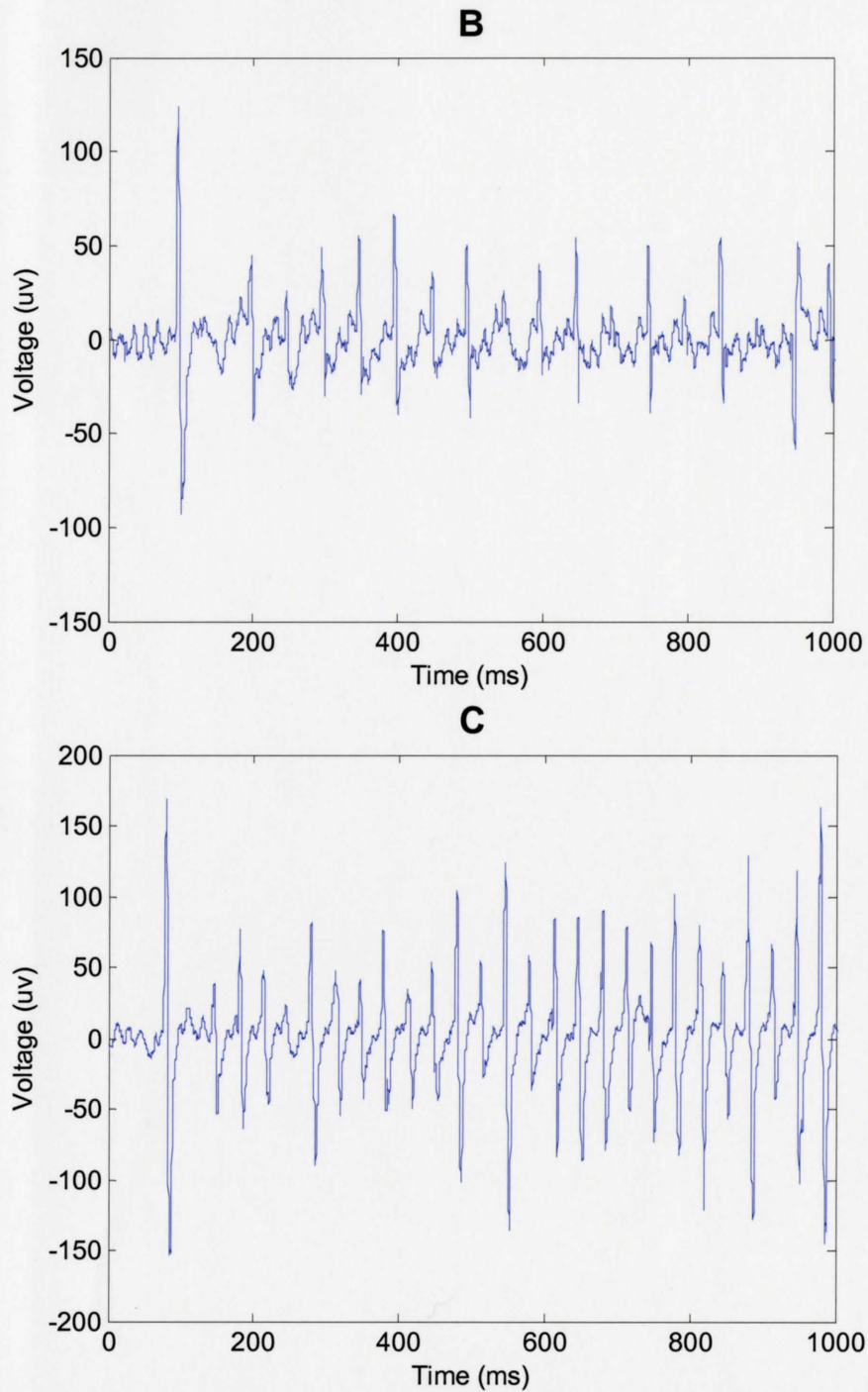

Figure 4-2: continued next page.

Figure 4-2: Response of subject 1 to A – 10 Hz, B – 20 Hz, C – 30 Hz. The degree of entrainment remains fairly consistent; 96% in A, to 71% in B, to 82% in C.

Figure 4-3: continued on next page.

Figure 4-3: Response of subject 2 to A – 10 Hz, B – 20 Hz, C – 30 Hz. The degree of entrainment decreases from 86% in A, to 51% in B, to 34% in C.

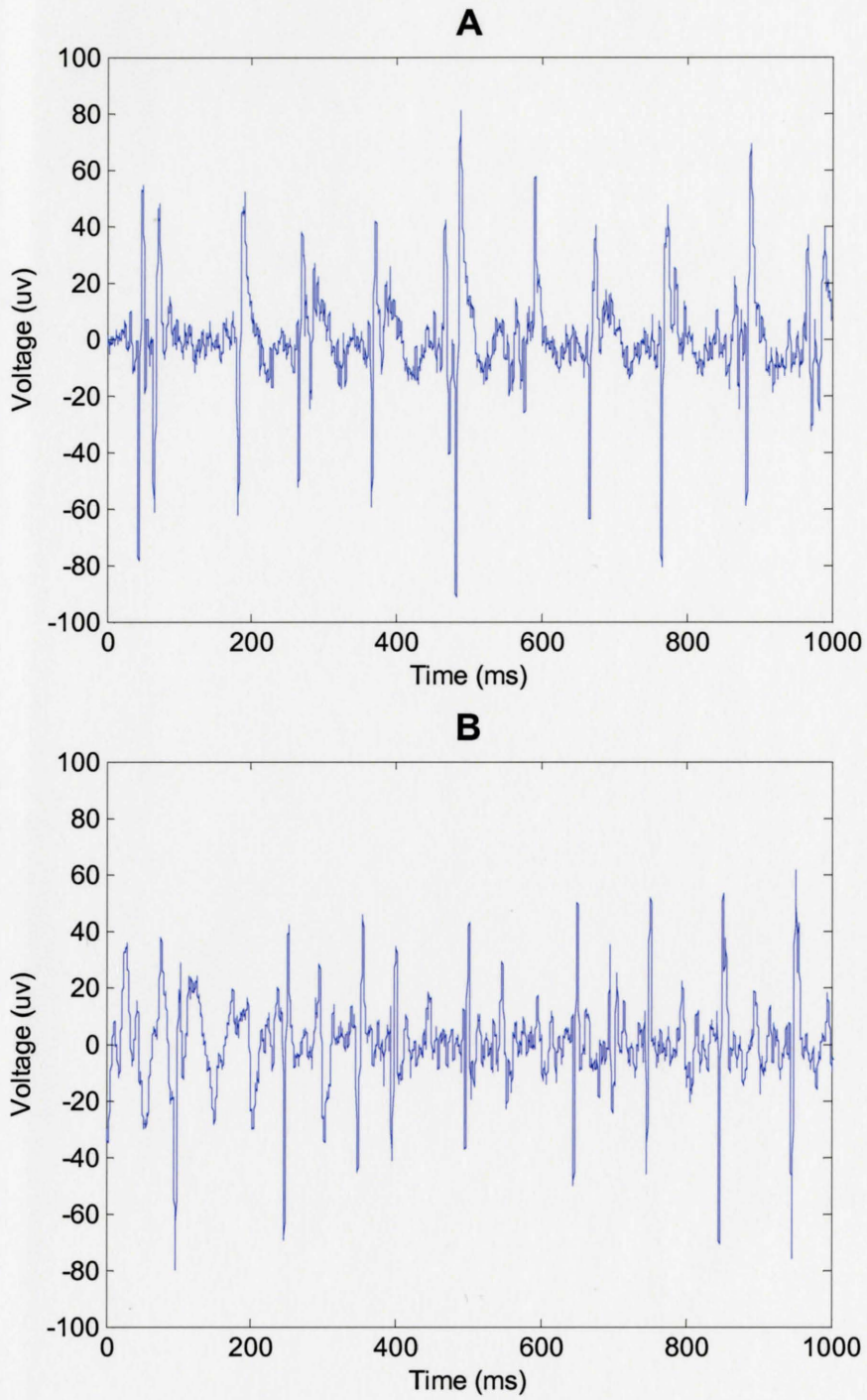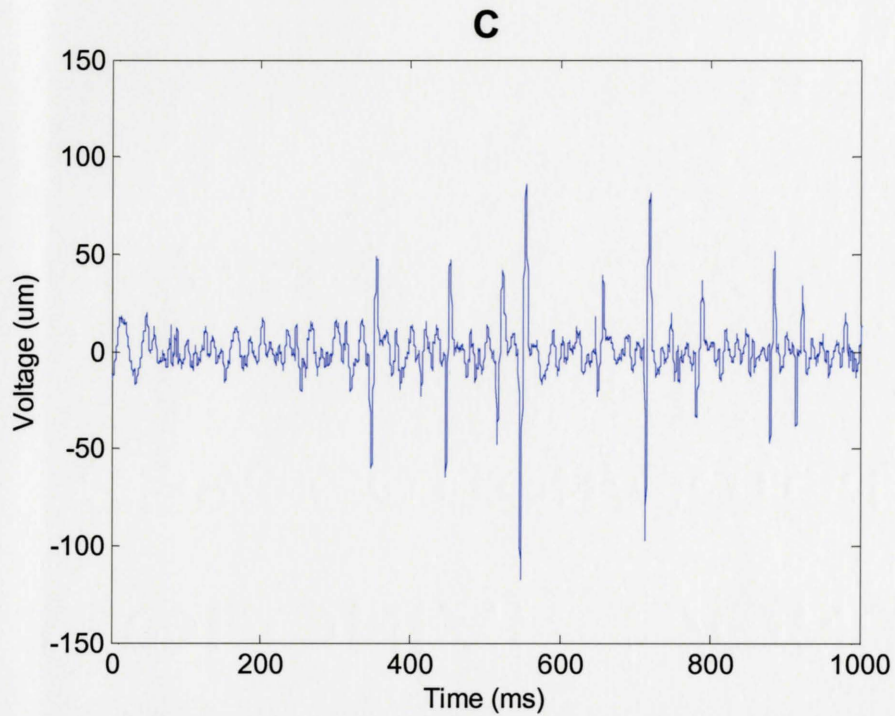Figure 4-4 and Table 4-1 represents the cumulative data for all trials at each frequency for each subject. The data points are the mean degree of entrainment per frequency per subject, and the error bars represent one standard deviation from the mean.

Table 4-1: Mean response entrainment and standard deviations for both subjects from 10-30 Hz.

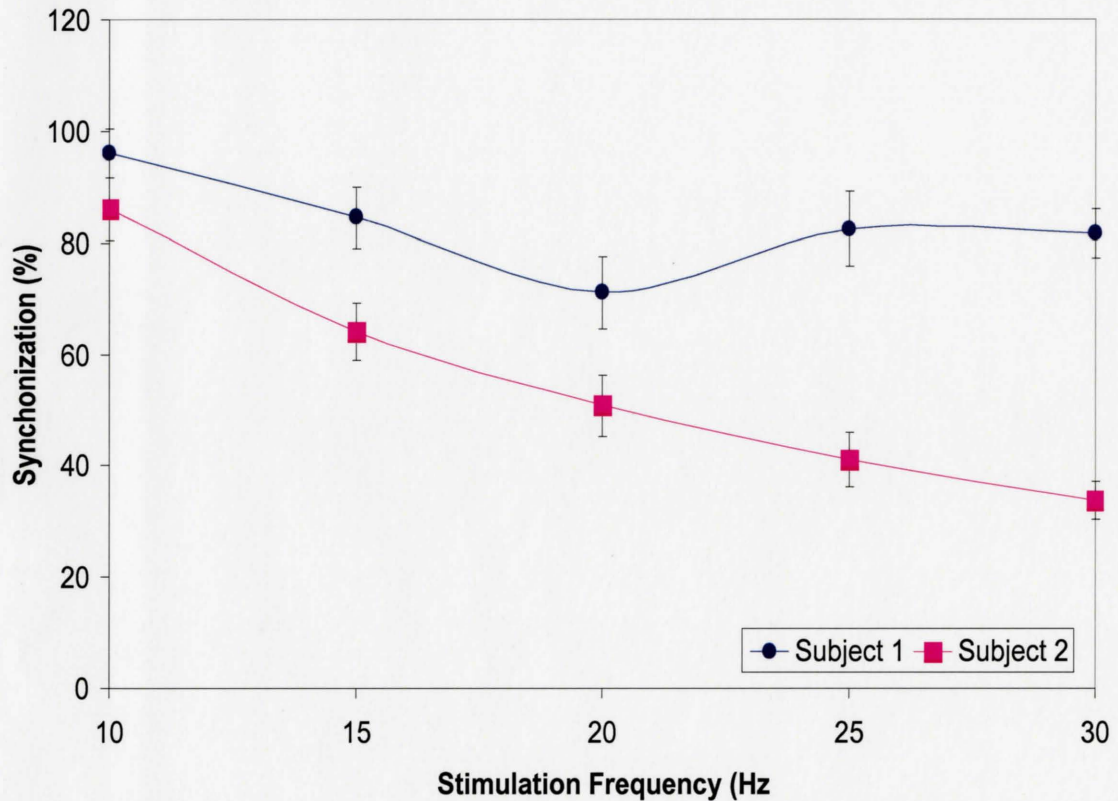|		10	15	20	25	30
	Frequency	10	15	20	25	30
Subject 1	Mean degree of entrainment	96	84	71	82	82
(25 years old)	Standard Deviation	4	4	6	6	4
Subject 2	Mean degree of entrainment	86	64	51	41	34
(63 Years Old)	Standard Deviation	5	5	4	5	2

Figure 4-4: Summary for the response entrainment results. The circle line represents subject 1; the square line represents subject 2. Subject 1 demonstrated a higher degree of entrainment for all vibration frequencies tested. Subject 2 also showed a steady decline in entrainment.

Note the degree of entrainment of the younger subject, subject 1, is higher than subject 2 over the entire range of frequencies tested, remaining near or above 80%, while subject 2 demonstrated an almost negative exponential decline in entrainment from slightly over 80% to below 40%. More importantly, both subjects demonstrated a high level of entrainment for 10 Hz vibrations. Subject one was even able to respond with a high degree of entrainment at higher frequencies, as seen in his 30 Hz vibration recordings. This is all in contrast to the H-reflex, which as mentioned during the background chapter, cannot be elicited at rates over 0.2-0.3 Hz, even though microneurographic work indicates that muscle spindles can fire in 1:1 response to vibrations of much higher frequencies.

4.3 Agonist and antagonist contractions

In this study, the response to slight isometric flexion, slight isometric extension, and relaxed wrist was recorded for 1s, 4mm, 10 and 30 Hz vibrations for both subjects. Again, 5-6 trials were conducted for each scenario (flexion, extension, and relaxed for 2 frequencies) and their mean peak to peak amplitude per response spike and mean degree of entrainment are summarized in Table 4-2. Typical results for subject 1 are shown in Figure 4-5 and Figure 4-6; and for subject 2, Figure 4-7 and Figure 4-8, for 10 and 30 Hz respectively.
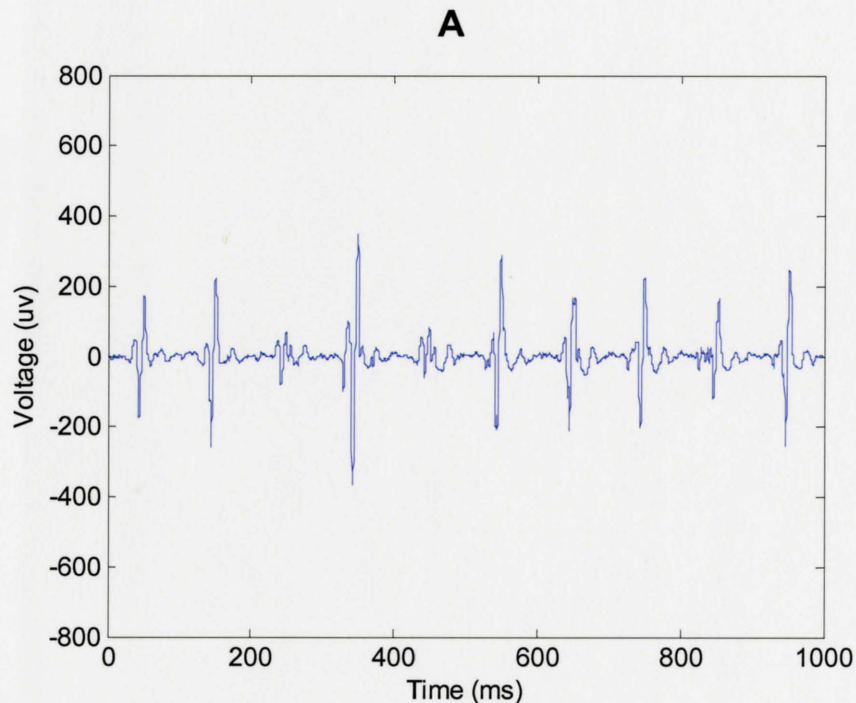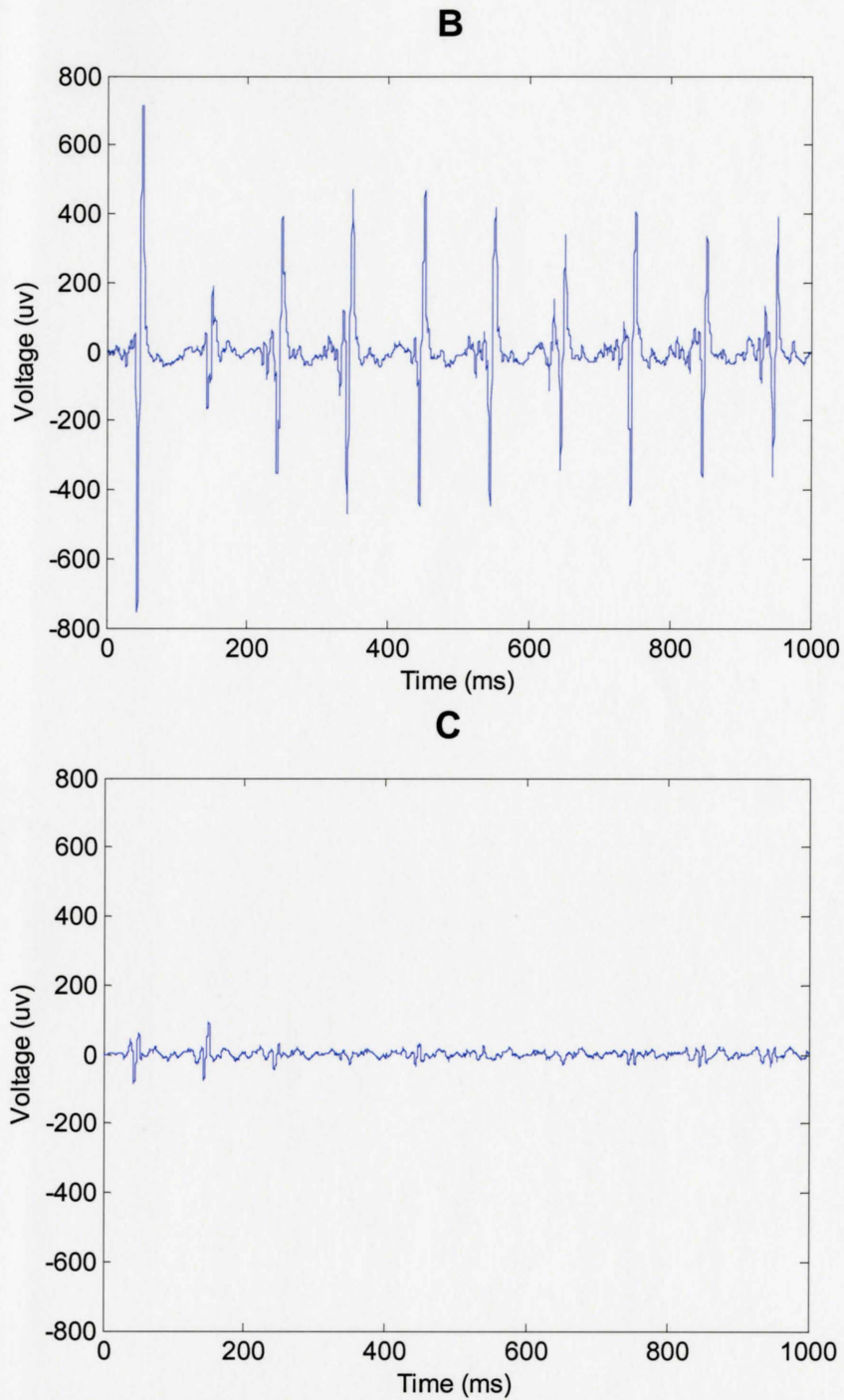

Figure 4-5: continued on next page.

Figure 4-5: Contraction results for subject 1 for a 4mm, 1s, 10 Hz vibration. A – for relaxed state, there was a 100% entrainment of response, and a 392±54 μv mean peak to peak response

spike amplitude. B – for slightly flexed wrist, there was a large increase in response amplitude, with mean 793±98 µv, and entrainment remained 100%. C – for slightly extended wrist, entrainment dropped to 90% and the mean amplitude per response to 79±15 µv.

As shown in the previous pilot study, both subjects demonstrate a high degree of response entrainment for 10 Hz vibrations, and this is also reflected in this study. Thus for subject 1 at 10 Hz, the most observable variation was the large change in mean response amplitude, nearly doubling for wrist flexion from relaxed state, and reducing to less than a fifth of the mean relaxed state amplitude for wrist extension.

Subject 1's response to 30 Hz vibration demonstrated not only a change in amplitude but also in degree of entrainment, with wrist flexion demonstrating an increase in both variables, while wrist extension reduces both.
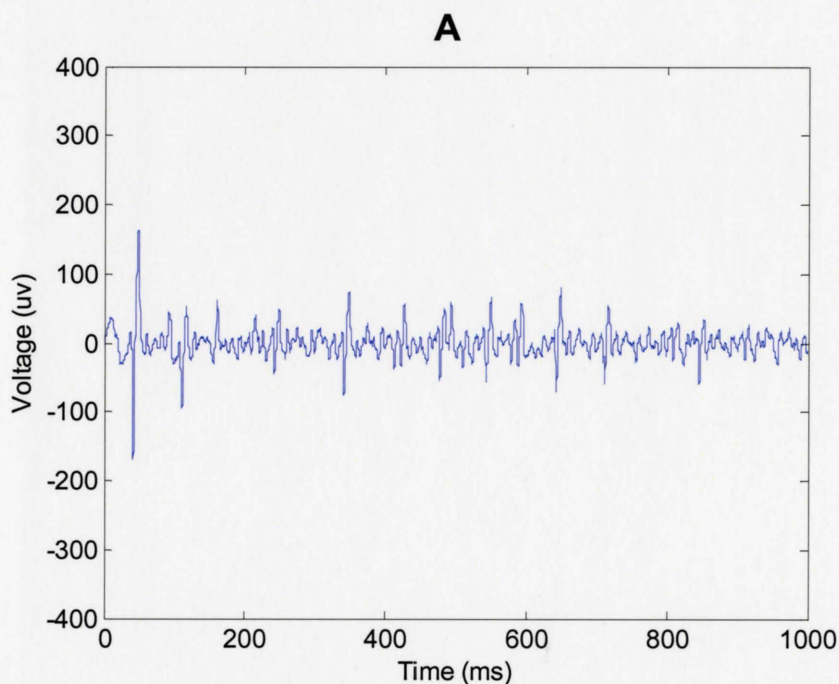

Figure 4-6: continued on the next page.
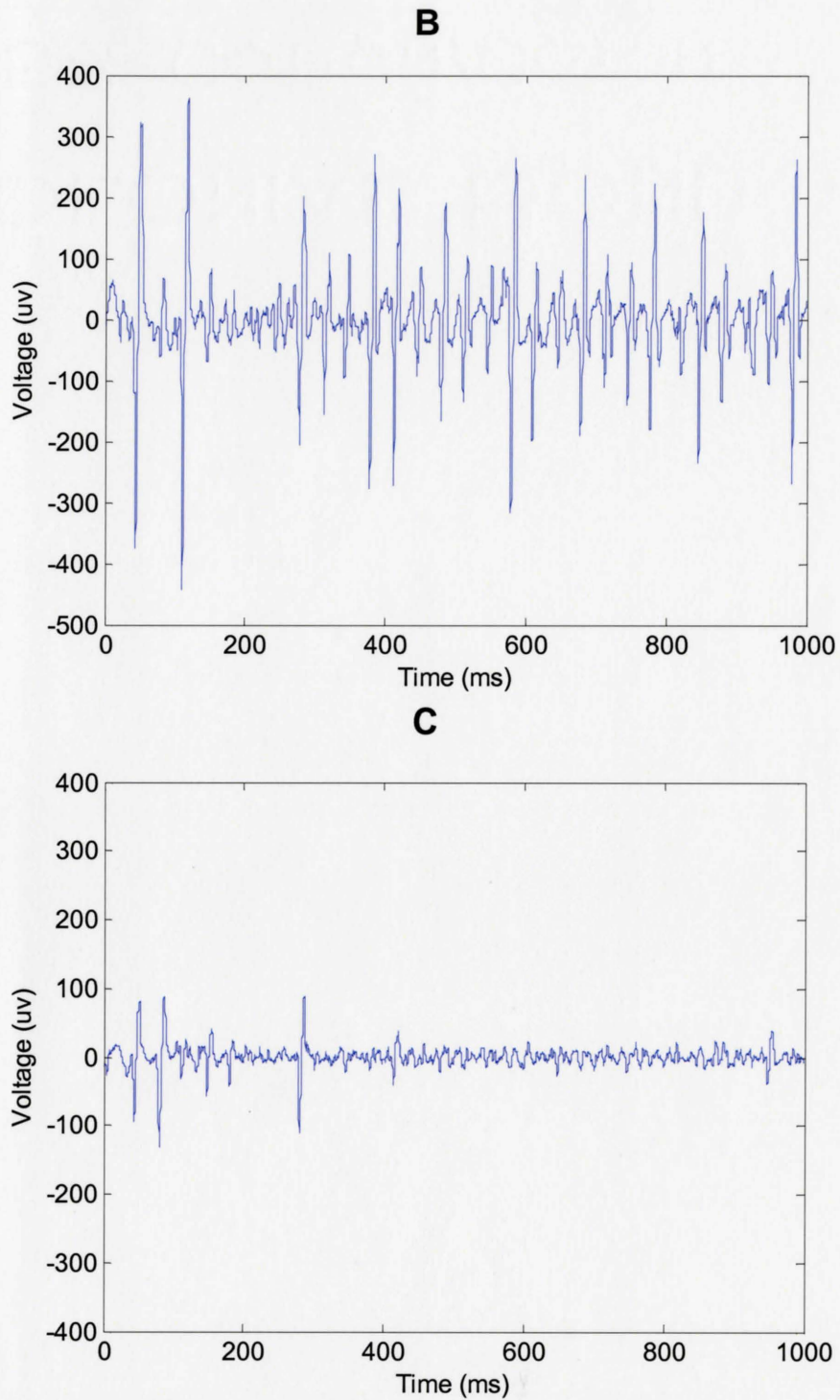
B

C

Figure 4-6: Contraction results for subject 1 for a 4mm, 1s, 30 Hz vibration. A – for relaxed

state, there was a 30% entrainment of response, and a 146±21 µv mean response spike amplitude. B – for slightly flexed wrist, mean response amplitude increased to 355±36 µv, and an increase in entrainment to 77%. C – for slightly extended wrist, entrainment dropped to 23% and the mean amplitude per response to 114±20 µv.

Subject 2 behaved similarly to subject 1 for the 10 Hz vibration. The degree of entrainment remained near 100%, and mean amplitude increased sharply for wrist flexion and decreased for wrist extension. Behaviour for 30 Hz vibration was not so similar to subject 1. Subject 2 demonstrated comparable mean response amplitudes for relax, wrist flexion, and wrist extension. There was however a much more pronounced change in the degree of entrainment in comparison to 10 Hz, and to subject 1's 30 Hz results, especially for wrist extension.

A

Figure 4-7: continued on next page.

Figure 4-7: Contraction results for subject 2 for a 4mm, 1s, 10 Hz vibration. A – for relaxed state (89±5 μv amplitude, 100% entrainment), B – slight wrist flexion (203±12 μv amplitude,

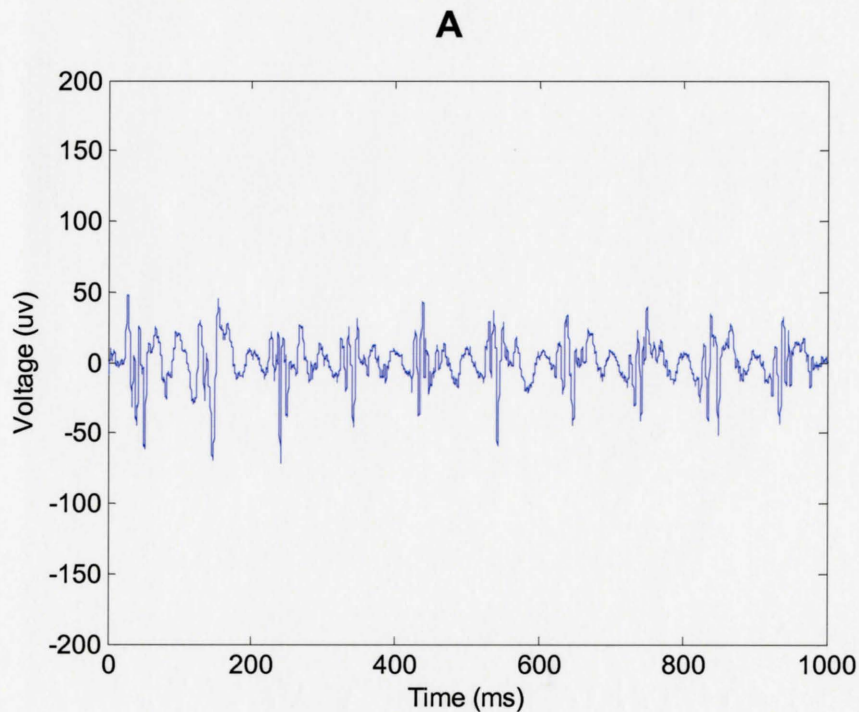**100% entrainment), C – slight wrist extension (71±9 μv amplitude, 80% entrainment).**

A
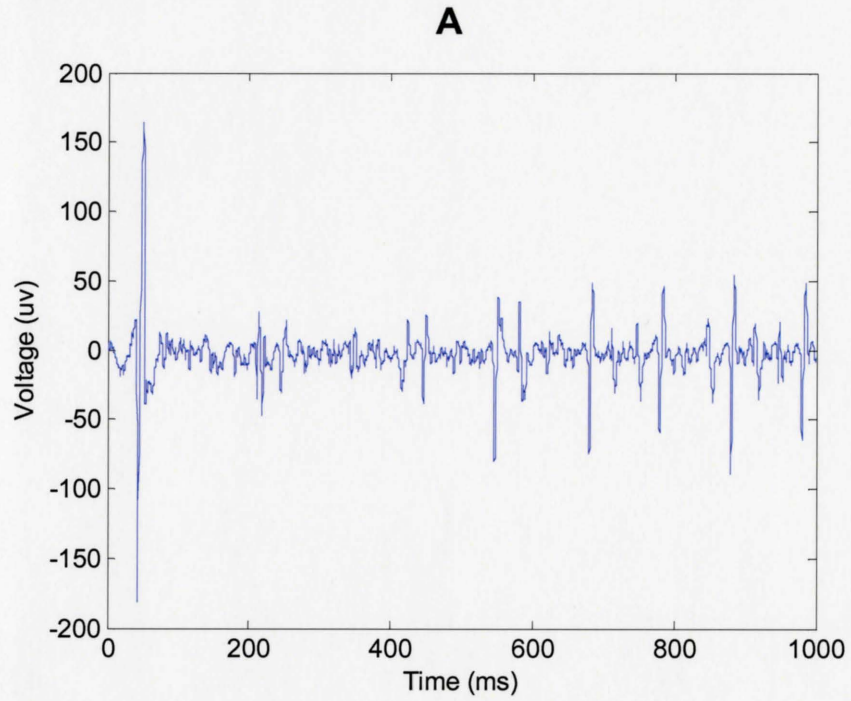
Figure 4-8: continued on next page.

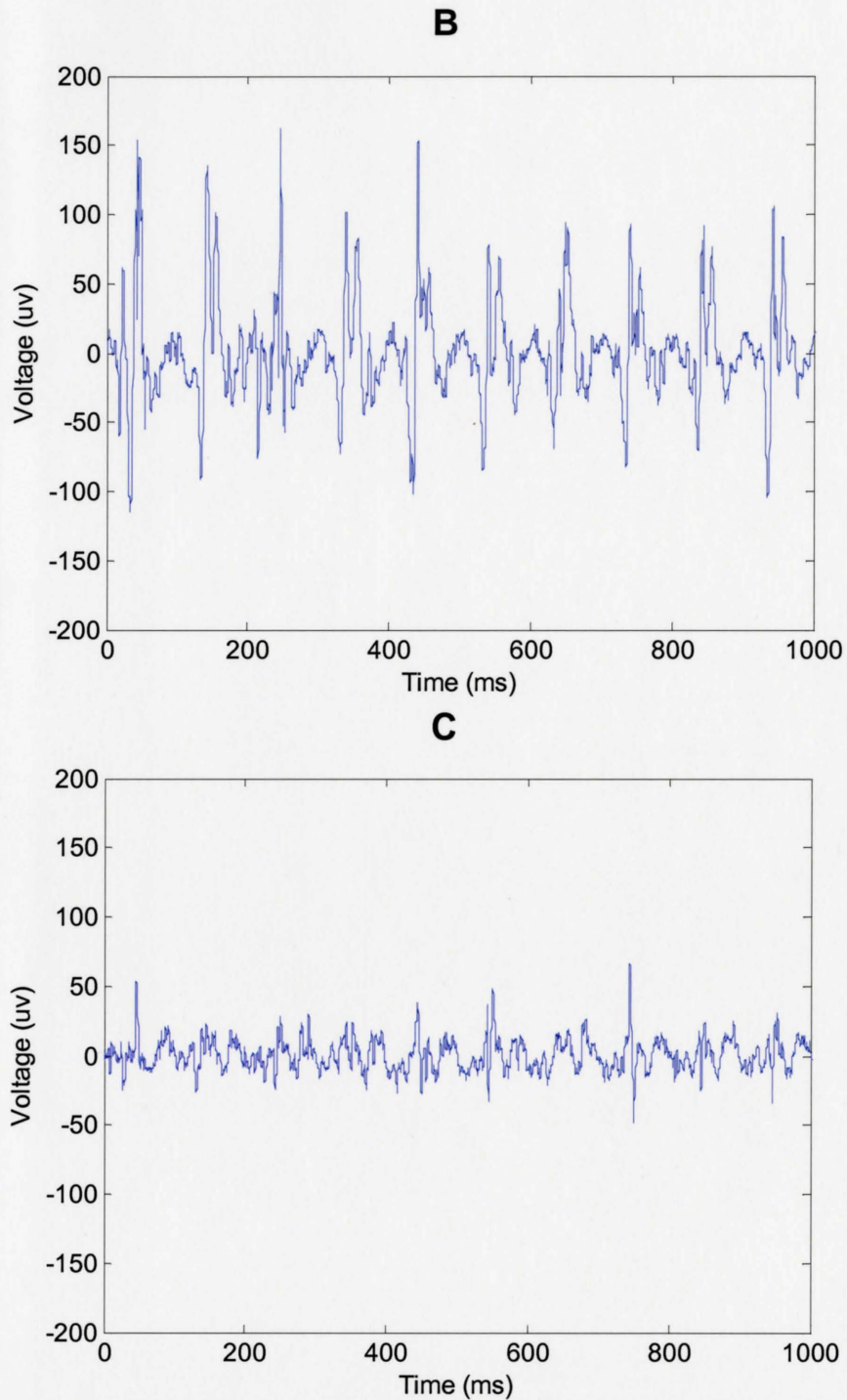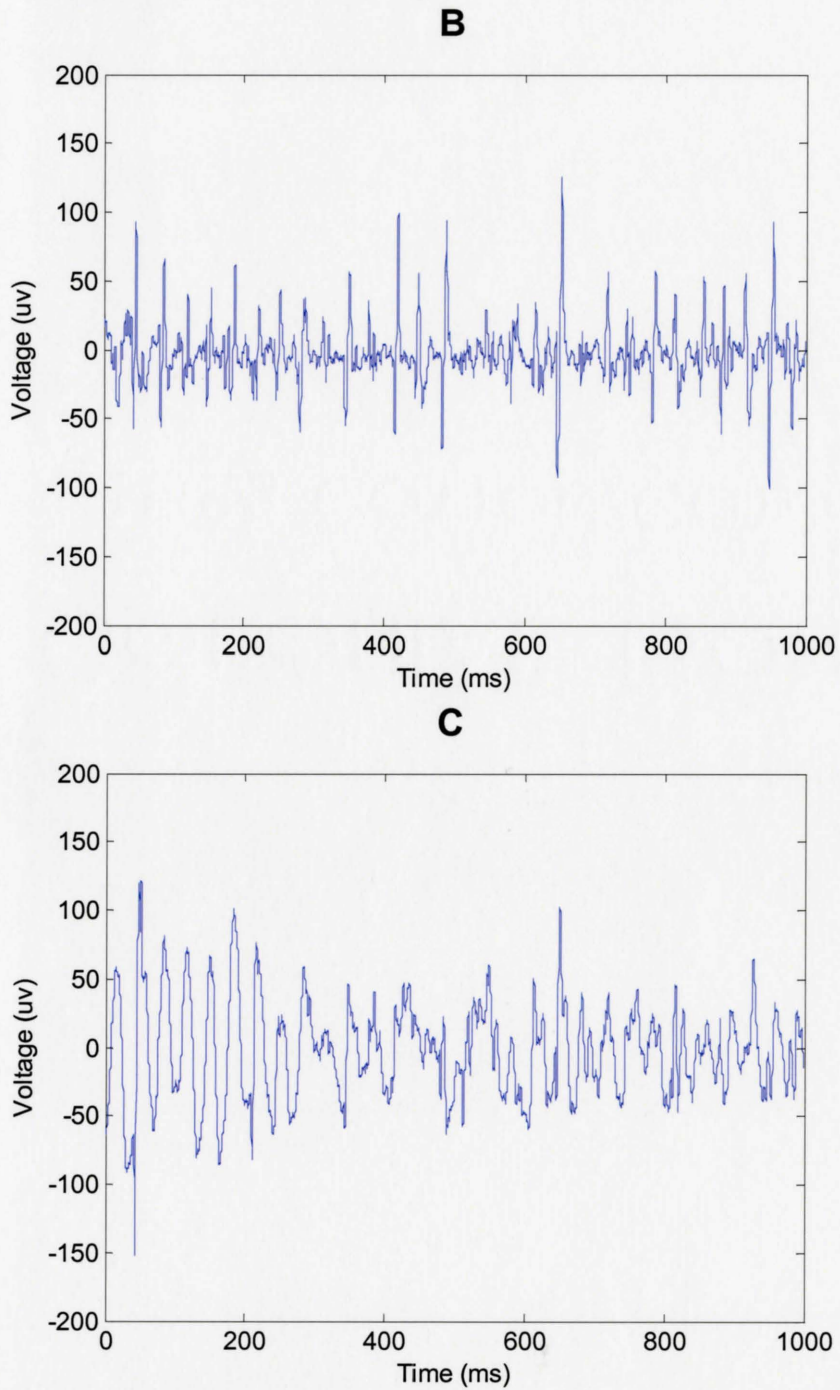**Figure 4-8: Contraction results for subject 2 for a 4mm, 1s, 30 Hz vibration. A – for relaxed state**

(114±21 µv amplitude, 37% entrainment), B – slight wrist flexion (109±9 µv amplitude, 73% entrainment), C – slight wrist extension (158±24 µv amplitude, 17% entrainment).

Table 4-2: Summary of contraction study results for both subjects (mean and standard error of amplitude of response spikes, and degree of entrainment at each vibration frequency).

			Relaxed	Slight Flexion	Slight Extension
Subject 1	10 Hz	Mean amplitude (µv)	392	793	79
		Standard error	55	98	15
		Degree of entrainment (%)	100	100	90
	30 Hz	Mean amplitude (µv)	146	355	114
		Standard error	21	36	20
		Degree of entrainment (%)	30	77	23
Subject 2	10 Hz	Mean amplitude (µv)	89	203	71
		Standard error	5	13	9
		Degree of entrainment	100	100	80
	30 Hz	Mean amplitude (µv)	114	109	158
		Standard error	21	9	25
		Degree of entrainment (%)	37	73	17

4.4   Separation of Ia and Ib pathways at low frequencies

This study was prompted by several test results obtained during the entrainment study at low vibration frequencies that showed responses with double spikes. These double spikes are separated by delays that were well within the typical delay that would occur between the taps in the vibration train.

The tests were done via a 1 s, 4 mm vibration of the FCR at 2, 4, 6, 8, and 10 Hz for both subjects. Our intent was to find the range of frequencies at which double responses were observable, as we have seen in Archambeault, de Bruin et al. (2006) and in our own single tap recordings that the occurrence of double responses does not simply increase with decreasing frequency, as single taps rarely elicit double responses (see Figure 1-7). Subject 1's results for 4 - 10 Hz are shown in Figure 4-9, followed by subject 2's results for 2 - 10 Hz in Figure 4-10.
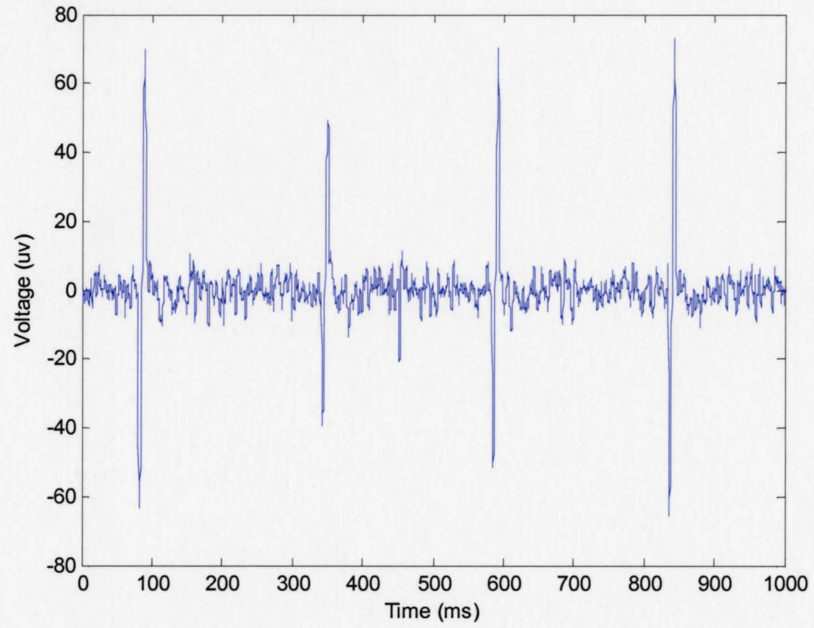
Figure 4-9: continued on next page.

Figure 4-9: Low frequency, 4 mm, 1 s, vibration recordings for subject 1. A – 4 Hz (no double spikes), B – 6 Hz (mean delay during double spikes was 21±1 ms), C – 8 Hz (mean 22±2 ms), D- 10 Hz (no double spikes).

The delay is calculated as the time between the mid-point of each spike in the double response (the mid-point being the zero crossing between the positive and negative phase of each spike). Subject 1 only demonstrated double spikes over a narrow range of vibration frequencies (just 6 and 8 Hz), with very consistent double spike responses at 6 Hz. The time delay was also consistent between these 2 frequencies. Entrainment remained close to 100% through the frequency range (with one missing response at 8 Hz), as was to be expected at such low vibration frequencies for both subjects. There does not seem to be any correlation between the amplitude of the 2 spikes in each double response; for some instances the first will be larger in amplitude, and the second is larger in other instances.

A
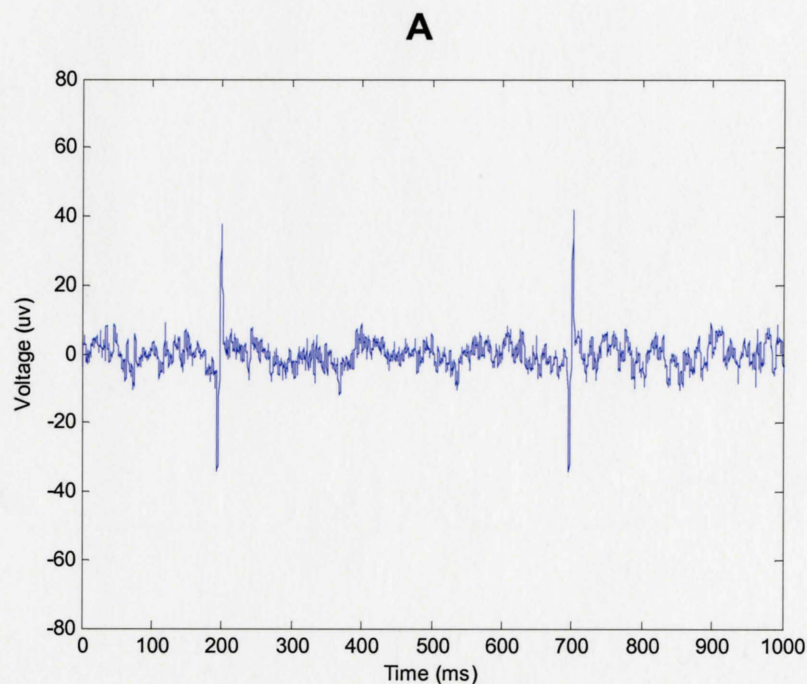
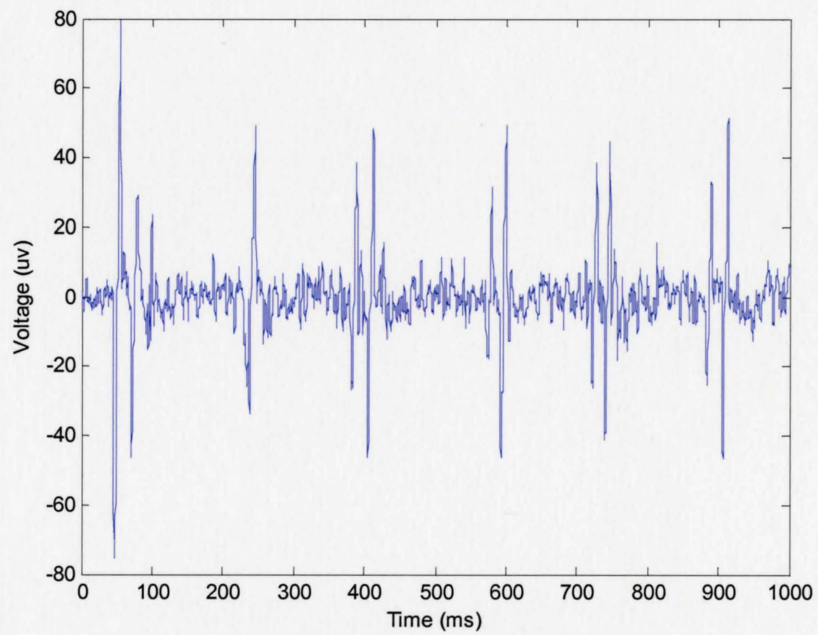**Figure 4-10: continued on next page.**

B
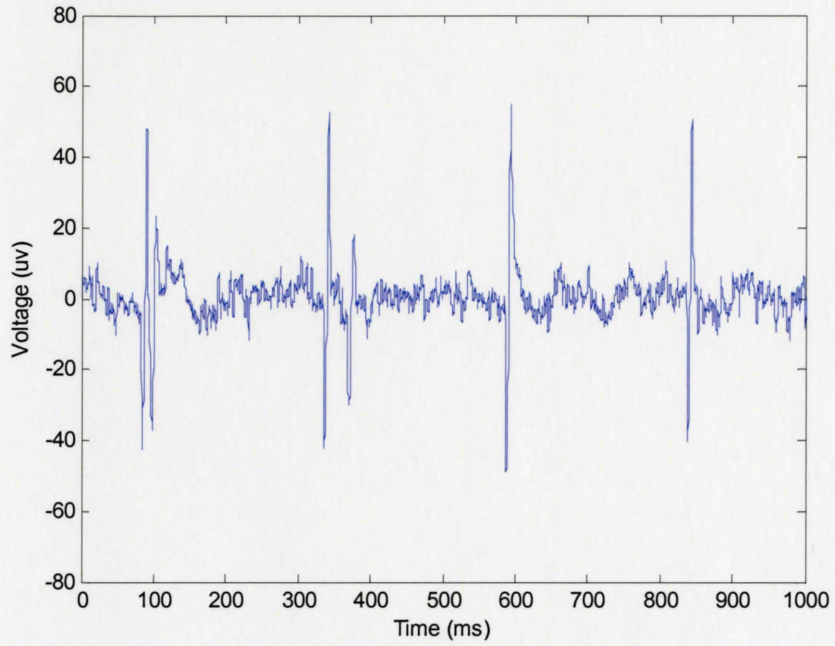
C
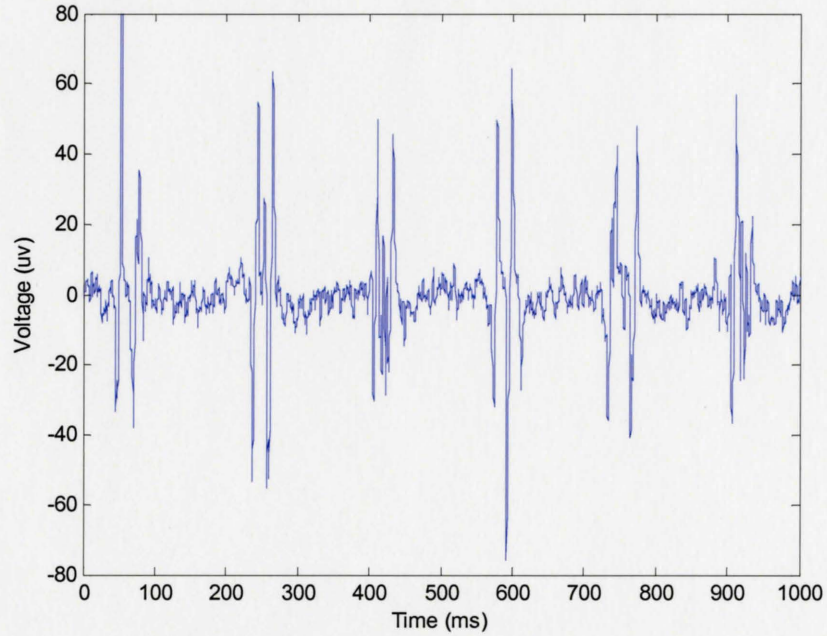
Figure 4-10: continued on next page.

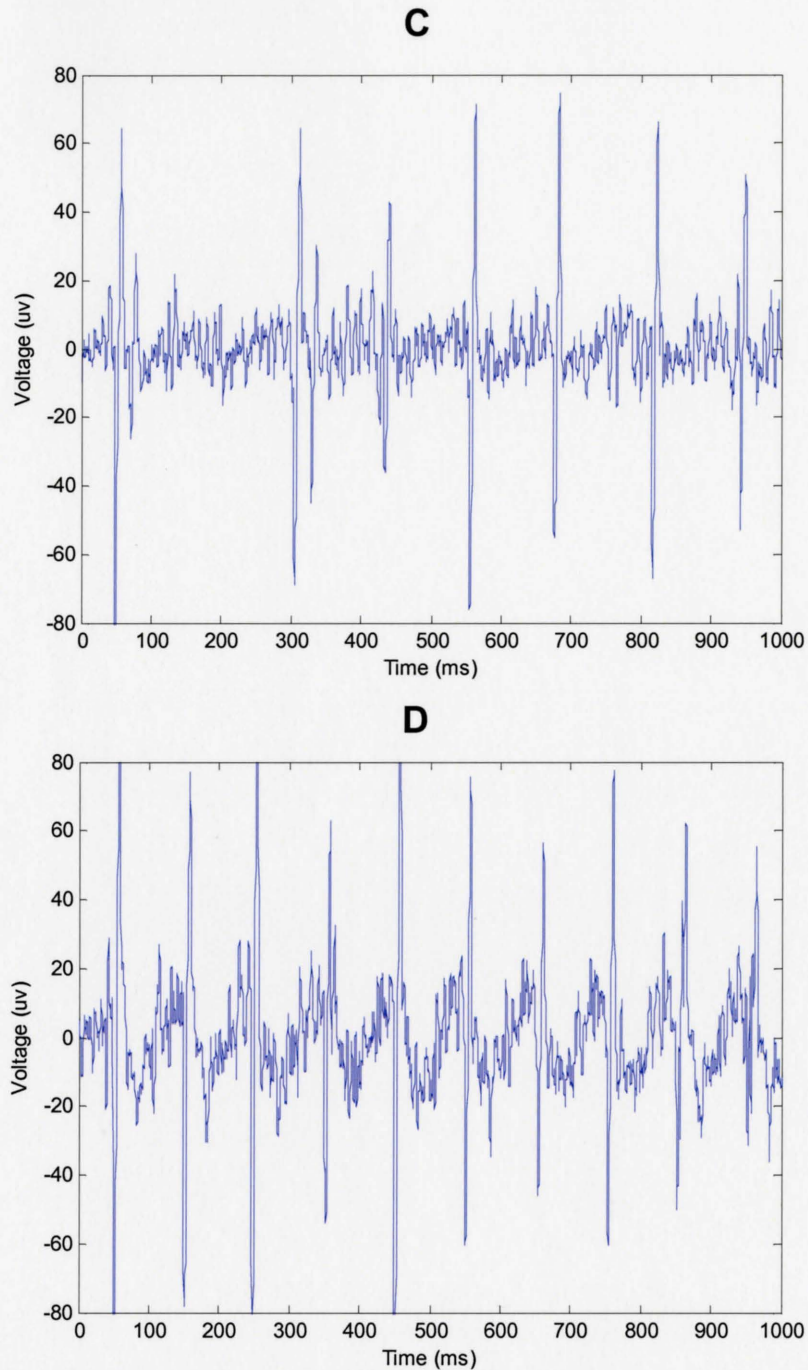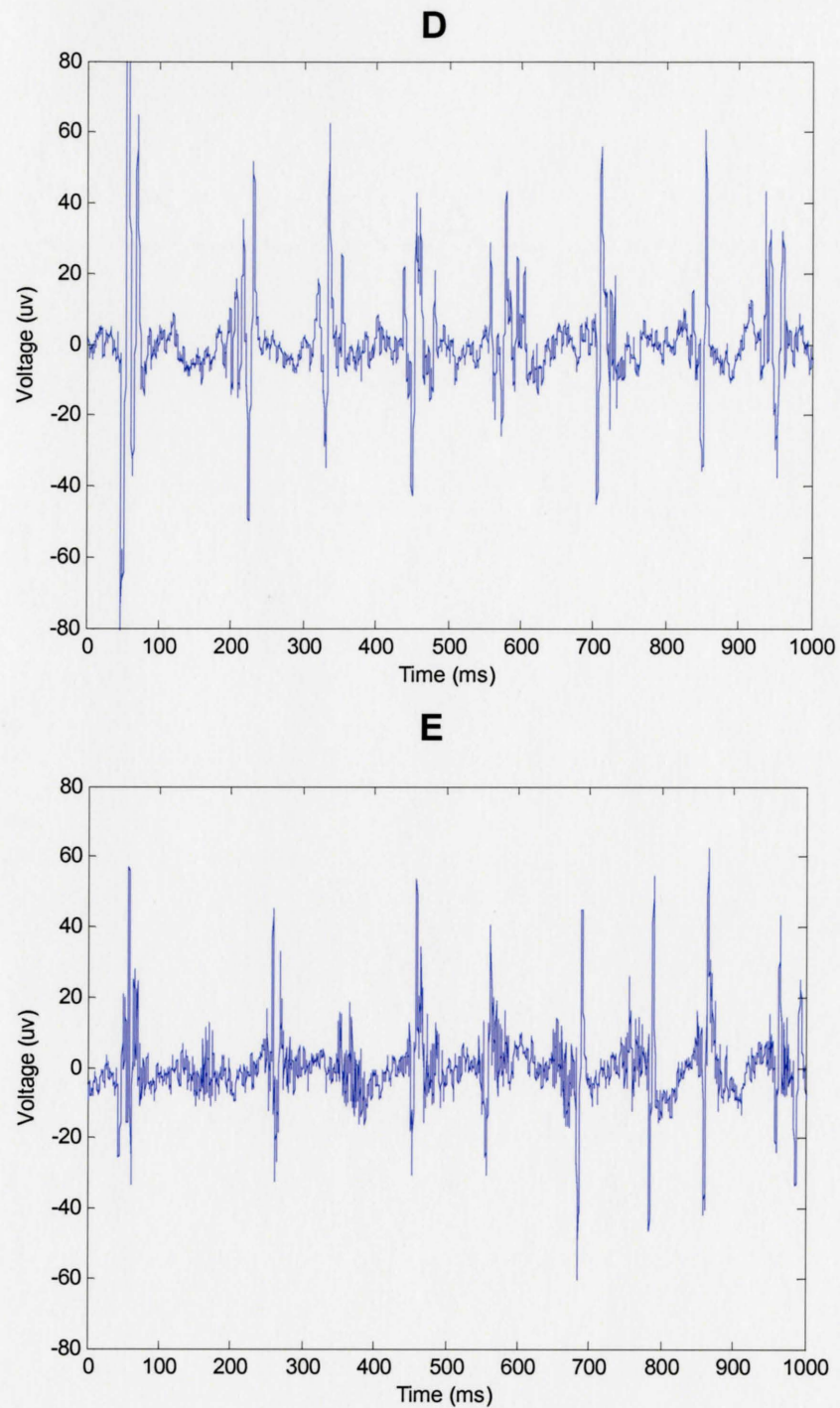**Figure 4-10: Low frequency, 4 mm, 1 s, vibration recordings for subject 2. A – 2 Hz (no double spikes), B – 4 Hz (mean delay 23±10 ms), C – 6 Hz (mean delay 24±2 ms), D- 8 Hz (mean delay**

18±2 ms), E – 10 Hz (mean delay 20±8 ms). Note the presence of double spikes at 4 Hz and 10 Hz, in contrast with subject 1.

Table 4-3: Summary of results for low frequency vibration.

	Vibration Frequency (Hz)	2	4	6	8	10
Subject 1	# of double responses	0	0	5	2	0
	Mean delay (ms)			21	22	
	Standard error			1	2	
Subject 2	# of double responses	0	2	6	7	2
	Mean delay (ms)		23	24	18	20
	Standard error		10	2	2	8

Subject 2 exhibited double spike responses over a larger range of vibration frequencies, featured consistently at 6 and 8 Hz, but also appearing, though with a lower frequency of occurrence, at 4 and 10 Hz. The delay during the double responses remained close to 20 ms. The results are summarized in Table 4-3.

In conjunction with these results, the conduction delay is calculated using the following formula for myelinated nerve fibres, found as formula 6.46 in (Plonsey and Barr 2000):

$$\Theta = 6d \qquad \text{m/sec (d in } \mu\text{m)}$$

Then, assuming that the length of a typical afferent fibre from the arm to the spinal cord is 1 m, the conduction delays are summarized in the following table.

Table 4-4: Calculation of delay due to conduction velocity differences for Ia and II afferent fibres.

	Ia	II
Axon Diameter (μm)	17	8
Conduction Velocity (m/s)	102	48
Time to travel 1 m (ms)	9.8	20.8

Thus we see that the contribution to the double response delay due to differences in conduction velocity is about 11 ms. Although from the data the delays between the two responses is roughly twice this, we could still attribute the two reflex responses to primary and secondary ending if the spinal connections for each are different (discussed in 4.5.3). Also, if the alpha MNs the Ia/II fibres innervate have different diameters, possibly due to a preferential innervation of II fibres to smaller motor units, an additional delay due to the difference in traveling time down the MN will contribute to the observed spike separation.

4.5   Discussion of Physiological Results

4.5.1 Degree of Entrainment

As explained during the background section, high frequency vibration should excite Ia fibres preferentially, as it induces quick changes of muscle length, and could fire the Ia afferents in a 1:1 fashion for frequencies near 80 Hz (Figure 1-14). While lower frequencies should excite II fibres to modulate their steady firing rate instead, as they rarely fire in a 1:1 fashion. Noting the low frequency experiments during the third pilot study, 10 Hz and above preferentially recruit Ia afferents for both subjects.

For this study using 10 Hz and above, assuming that MSs are able to fire 1:1 at high frequencies, and that tendon vibration could elicit such behaviour (both alluded to in microneurographic work), there seem to be varying degrees of innate spinal inhibition (independent of conditioning stimuli such as agonist/antagonist contraction) which prevent certain subjects from entraining at higher vibration frequencies (subject 2 demonstrated very low entrainment for 30 Hz, while subject one is nearly 100% at that same frequency). One possible explanation could be age, as the H-reflex has been shown to decrease in amplitude with age due to a variety of reasons (Kido, Tanaka et al. 2004), one being a possible decline in nerve potential amplitude (Rivner, Swift et al. 2001), thereby reducing the excitatory effects of Ia afferent fibres. It is possible that this decrease has reduced the response spike amplitude to below the noise floor of this system, hence rendering them undetectable.

4.5.2   Agonist and Antagonist Contractions

The excitatory and inhibitory effects of agonist and antagonist contractions on the H-reflex response amplitude have already been shown. This study reveals that not only is the amplitude of response affected but also the response time of the entire simple reflex arc, creating changes in degree of entrainment between stimulus and response. This could possibly be also attributed to presynaptic inhibition, where Ia axon endings are inhibited, reducing the excitatory efficacy of each MS, thus depressing some stimuli to below response threshold.

Noting the appearance of only a few but long duration gaps in response in subject two's 30 Hz recordings, in contrast with an even distribution of smaller gaps, it is possible that the vibration, at the spinal level, is a cumulative stimulus, as it requires the temporal summation of Ia afferent firings. Perhaps the vibration stimulus has to "build up" in the spinal cord during inhibitory contractions in order to meet the threshold. In the same way, an increase in entrainment could be due to lowering of response thresholds at the spinal cord, where a response requires fewer vibration stimuli (fewer taps).

4.5.3   Separation of Ia/II Pathways

Since not all of the delay can be attributed to conduction velocity differences, it is possible that the II pathway is more oligosynaptic than the Ia pathway (Nardone and Schieppati 2005). The same has been said about the H-reflex/tendon tap in general, that the contributions of oligosynaptic pathways elongate the response (more for mechanical stimuli than the electrical H-reflex) to longer than a MN stimulated M-wave (Burke,

Gandevia et al. 1984). From the limited data, we see that the delay is fairly consistent, and that methodologically we are able to consistently elicit double responses on a subject's cross-over frequency range is known. Thus further testing might be able to narrow down the possible mechanisms of the double spike responses.

CHAPTER 5
CONCLUSIONS

5.1 Summary

We had developed this system and its associated experimental protocols in hope that we may be able to further explore human reflex physiology using vibration. Along those lines some thought was given to improving the ease of use, reliability, and accuracy of the existing clinical and research methodologies such as the electrical H-reflex, microneurography, and EMG RMS level, while providing a more balanced picture of the simple reflex arc in response to vibration stimuli.

In regard to ease of use, the surface EMG capture and processing techniques utilized by this system is of definite advantage over traditional microneedle techniques used in microneurographical studies. Such studies require the careful and often subjective classification of the fibre currently in contact before any experiments can begin, not to mention the highly invasive nature of the technique. Even in comparison to H-reflex studies, a lack of fully programmable stimulators prevents the use of automated, easily repeatable experimental protocols. The integration of various control parameters using LabVIEW allows for much more streamlined experimental protocols, which may even allow for use by clinicians not familiar with the technical details of the system. The use of LabVIEW also allows for future expansion, such as the triggering of electrical stimuli, which has already been done in a previous work Archambeault, de Bruin et al. (2006).

One aspect of reliability that has been improved is the verification of motor compliance, which is left undone for most vibration studies. By choosing a motor with a high maximum force, we ensure that the motor is compliant to the tested motion

trajectories under varying load, even though the compliance may be lacking to strict high frequency sinusoids for this particular model. Also, the reduction techniques used on the major noise sources, 60 Hz power line and vibration artifact noise, in post processing, allow for uncontaminated time domain views of any elicited responses, from which a variety of other statistical measures could be derived accurately.

Physiologically, this system opens up many different avenues of research into human spinal reflexes. We investigated several as pilot projects: (i) degree of entrainment between stimulus and response, (ii) effect of agonist and antagonist contractions, (iii) observable separation of Ia and II pathways. The degree of entrainment varied between subjects, even for the relatively low (10 to 30 Hz) vibration frequencies used. The younger subject demonstrated a much higher degree of entrainment at higher frequencies than the significantly older subject, supporting existing evidence that spinal reflexes diminish with age.

The effect of slight agonist and antagonist contractions of the wrist showed results in line with what was already established in H-reflex presynaptic inhibition work; that agonist activity had overall excitatory effects, and antagonist activity had overall inhibitory effects. How these conditioning stimuli affected the 2 parameters being measured - individual spike response amplitude, and degree of entrainment - varied between the subjects, with subject one tending to demonstrate changes in response amplitude while subject two showing large changes in degree of entrainment.

We encountered a possible separation of Ia\II pathways during low vibration frequency experiments; where double spike responses occurred with high regularity. Further experiments undertaken at vibration frequencies below 10 Hz showed a consistent delay between these pairs of double spikes, suggesting a common physiological mechanism as its cause. The range of frequencies at which these double spikes occurred, however, were different between the subjects.

The relative ease with which these initial pilot experiments were done using this system, and the consistent, reliable, and physiologically relevant results that it captures, solidify it as a valuable tool in the exploration of human spinal reflexes.

5.2   Future Work

There are a few areas where the equipment and post processing could be improved upon in terms of efficacy, versatility, and ease of use.

The linear servomotor chosen was not able to generate reliable vibrations much beyond 40 Hz. A motor with high frequency capabilities may improve the motion compliance at lower frequencies, eliminating the need to use pseudo-sinusoids. Also, custom position tracking capabilities could be used to record motor position during experimental protocols. Currently, position tracking is available only when using the motor's own software, independent from LabVIEW.

A phase coherent subtractive filter was chosen as it was simple to implement, and its effects were easily verifiable. This simplicity, however, does have the drawback that the noise shape must be visually observable in the time domain; in essence the noise must dominate the signal, or otherwise be recorded separately (as is the case with 60 Hz power line noise) for the filter to generate a well fitting noise signal to be subtracted. While this technique has been tremendously useful for many sets of data recorded during this project, non-time domain techniques, such as advanced digital domain filtering, should be explored to remove these noise sources when they are not detectable visually. Further more, pattern recognition could be used to locate and identify individual stretch responses, versus fully relying on the phase locked entrainment of the responses and visual inspection.

On the physiology side, it will be important for these pilot studies to be extended to larger populations, perhaps even to diseased populations. The variables investigated, degree of entrainment in particular, could be further refined as a possible quantitative measure of spasticity, where currently only qualitative clinical scales exist.

CHAPTER 6
REFERENCES

Albert, F., M. Bergenheim, et al. (2006). "The Ia afferent feedback of a given movement evokes the illusion of the same movement when returned to the subject via muscle tendon vibration." Exp Brain Res **172**(2): 163-74.

Archambeault, M., H. de Bruin, et al. (2006). "Tendon reflexes elicited using a computer controlled linear motor tendon hammer." Conf Proc IEEE Eng Med Biol Soc **1**: 5068-71.

Aymard, C., B. Decchi, et al. (1997). "Recurrent inhibition between motor nuclei innervating opposing wrist muscles in the human upper limb." J Physiol **499** (Pt 1): 267-82.

Banks, R. W. (2006). "An allometric analysis of the number of muscle spindles in mammalian skeletal muscles." J Anat **208**(6): 753-68.

Basmajian, J. V. (1980). "Electromyography--dynamic gross anatomy: a review." Am J Anat **159**(3): 245-60.

Bonnet, M., J. Decety, et al. (1997). "Mental simulation of an action modulates the excitability of spinal reflex pathways in man." Brain Res Cogn Brain Res **5**(3): 221-8.

Burke, D. (2002). "Effects of activity on axonal excitability: implications for motor control studies." Adv Exp Med Biol **508**: 33-7.

Burke, D., S. C. Gandevia, et al. (1983). "The afferent volleys responsible for spinal proprioceptive reflexes in man." J Physiol **339**: 535-52.

Burke, D., S. C. Gandevia, et al. (1984). "Monosynaptic and oligosynaptic contributions to human ankle jerk and H-reflex." J Neurophysiol **52**(3): 435-48.

Cheng, J., J. D. Brooke, et al. (1998). "Crossed inhibition of the soleus H reflex during passive pedalling movement." Brain Res **779**(1-2): 280-4.

Christie, A., S. Lester, et al. (2004). "Reliability of a new measure of H-reflex excitability." Clin Neurophysiol **115**(1): 116-23.

Cody, F. W., N. C. Henley, et al. (1998). "Phasic and tonic reflexes evoked in human antagonistic wrist muscles by tendon vibration." Electroencephalogr Clin Neurophysiol **109**(1): 24-35.

Courtine, G., A. M. De Nunzio, et al. (2007). "Stance- and locomotion-dependent processing of vibration-induced proprioceptive inflow from multiple muscles in humans." J Neurophysiol 97(1): 772-9.

Crone, C. and J. Nielsen (1989). "Methodological implications of the post activation depression of the soleus H-reflex in man." Exp Brain Res 78(1): 28-32.

De Luca, C. J., R. S. LeFever, et al. (1982). "Behaviour of human motor units in different muscles during linearly varying contractions." J Physiol 329: 113-28.

Delliaux, S. and Y. Jammes (2006). "Effects of hypoxia on muscle response to tendon vibration in humans." Muscle Nerve 34(6): 754-61.

Fallon, J. B. and V. G. Macefield (2007). "Vibration sensitivity of human muscle spindles and Golgi tendon organs." Muscle Nerve 36(1): 21-9.

Freund, H. J., H. J. Budingen, et al. (1975). "Activity of single motor units from human forearm muscles during voluntary isometric contractions." J Neurophysiol 38(4): 933-46.

Fu, W. (2005). Modulation of the Ia input: Motoneurone outpur relationship of human flexor carpi radialis during muscle contraction. Electrical and Computer Engineering. Hamilton, McMaster University. M.ASc.

Fu, W., H. de Bruin, et al. (2004). Modulation of the Ia input: motoneurone output relationship of human flexor carpi radialis during muscle contraction. 17th Bien Int EURASIP Conf Biosignal, Brno, Czech Republic.

Gosgnach, S., J. Quevedo, et al. (2000). "Depression of group Ia monosynaptic EPSPs in cat hindlimb motoneurones during fictive locomotion." J Physiol 526 Pt 3: 639-52.

Guyton, A. and J. Hall (2006). Textbook of Medical Physiology. Philadelphia, Elsevier Inc.: 81.

Guyton, A. and J. Hall (2006). Textbook of Medical Physiology. Philadelphia, Elsevier Inc.: 89.

Guyton, A. and J. Hall (2006). Textbook of Medical Physiology. Philadelphia, Elsevier Inc.: 679.

Guyton, A. and J. Hall (2006). Textbook of Medical Physiology. Philadelphia, Elsevier Inc.: 674.

Henneman, E. and L. Mendell (1981). Handbook of Physiology. Bethesda, American Physiological Society: 423-507.

Henneman, E., G. Somjen, et al. (1965). "Excitability and inhibitability of motoneurons of different sizes." J Neurophysiol 28(3): 599-620.

Hoffmann, P. (1952). "Short review on the relations of reflex research by the electrical method in man and animals." Experientia 8(10): 371-5.

Hultborn, H., M. Illert, et al. (1996). "On the mechanism of the post-activation depression of the H-reflex in human subjects." Exp Brain Res 108(3): 450-62.

Katz, R. and E. Pierrot-Deseilligny (1999). "Recurrent inhibition in humans." Prog Neurobiol 57(3): 325-55.

Kido, A., N. Tanaka, et al. (2004). "Spinal excitation and inhibition decrease as humans age." Can J Physiol Pharmacol 82(4): 238-48.

Kleissen, R. F., J. H. Buurke, et al. (1998). "Electromyography in the biomechanical analysis of human movement and its clinical application." Gait Posture 8(2): 143-158.

Kohn, A. F., M. K. Floeter, et al. (1997). "Presynaptic inhibition compared with homosynaptic depression as an explanation for soleus H-reflex depression in humans." Exp Brain Res 116(2): 375-80.

Kokkorogiannis, T. (2004). "Somatic and intramuscular distribution of muscle spindles and their relation to muscular angiotypes." J Theor Biol 229(2): 263-80.

McIlroy, W. E., D. F. Collins, et al. (1992). "Movement features and H-reflex modulation. II. Passive rotation, movement velocity and single leg movement." Brain Res 582(1): 85-93.

Misiaszek, J. E. (2003). "The H-reflex as a tool in neurophysiology: its limitations and uses in understanding nervous system function." Muscle Nerve 28(2): 144-60.

Nardone, A. and M. Schieppati (2005). "Reflex contribution of spindle group Ia and II afferent input to leg muscle spasticity as revealed by tendon vibration in hemiparesis." Clin Neurophysiol 116(6): 1370-81.

Pierrot-Deseilligny, E. (1997). "Assessing changes in presynaptic inhibition of Ia afferents during movement in humans." J Neurosci Methods 74(2): 189-99.

Pierrot-Deseilligny, E. and D. Mazevet (2000). "The monosynaptic reflex: a tool to investigate motor control in humans. Interest and limits." Neurophysiol Clin **30**(2): 67-80.

Plonsey, R. and R. C. Barr (2000). Bioelectricity: A Quantitative Approach. New York, NY, Kluwer Academic/Plenum Publishers.

Rivner, M. H., T. R. Swift, et al. (2001). "Influence of age and height on nerve conduction." Muscle Nerve **24**(9): 1134-41.

Roll, J. P., J. P. Vedel, et al. (1989). "Alteration of proprioceptive messages induced by tendon vibration in man: a microneurographic study." Exp Brain Res **76**(1): 213-22.

Rossi, A., B. Decchi, et al. (1999). "Presynaptic excitability changes of group Ia fibres to muscle nociceptive stimulation in humans." Brain Res **818**(1): 12-22.

Rudomin, P. and R. F. Schmidt (1999). "Presynaptic inhibition in the vertebrate spinal cord revisited." Exp Brain Res **129**(1): 1-37.

Tortora, G. J. and B. Derrickson (2006). Motor Units. Principles of Anatomy and Physiology. Hoboken, NJ, John Wiley & Sons, Inc.: 309.

Voerman, G. E., M. Gregoric, et al. (2005). "Neurophysiological methods for the assessment of spasticity: the Hoffmann reflex, the tendon reflex, and the stretch reflex." Disabil Rehabil **27**(1-2): 33-68.

Yablon, S. A. and D. S. Stokic (2004). "Neurophysiologic evaluation of spastic hypertonia: implications for management of the patient with the intrathecal baclofen pump." Am J Phys Med Rehabil **83**(10 Suppl): S10-8.